ILLINOIS

UNIVERSITY OF ILLINOIS AT URBANA-CHAMPAIGN

-

PRODUCTION NOTE

University of Illinois at
Urbana-Champaign Library
Large-scale Digitization Project, 2007.

UNIVERSITY OF ILLINOIS
COLLEGE OF ENGINEERING

ENGINEERING EXPERIMENT STATION
BULLETIN 504

CRACKING OF CONCRETE

by
D. Naus
H. M. Rejali
J. L. Lott
C. E. Kesler

ENGINEERING EXPERIMENT STATION
BULLETIN 504

CRACKING OF CONCRETE

by

D. Naus
Instructor
Theoretical and Applied Mechanics
University of Illinois

H. M. Rejali
Research and Development Engineer
Combustion Engineering, Inc.
Windsor, Connecticut

J. L. Lott
Materials Research Engineer
U.S. Army Construction Engineering
Research Laboratory

C. E. Kesler
Professor
Theoretical and Applied Mechanics,
Civil Engineering
University of Illinois

Price: $3.00

Prepared as part of an investigation
conducted by
The Engineering Experiment Station
University of Illinois
in cooperation with
The State of Illinois
Division of Highways
and
The U.S. Department of Transportation
Federal Highway Administration
Bureau of Public Roads
Project IHR-92
Cracking of Concrete
Illinois Cooperative Highway Research Program
Series No. 115

Edited by

Virginia J. Griffin

REQUESTS FOR THIS PUBLICATION should be addressed to Engineering Publications Office, 112 Engineering Hall, University of Illinois, Urbana 61801. On your order refer to the Bulletin number on the front cover.

UNIVERSITY OF ILLINOIS BULLETIN
Volume 68, Number 5; August 12, 1970. Published twelve times each month by the University of Illinois. Entered as second-class matter December 11, 1912, at the post office at Urbana, Illinois, under the Act of August 24, 1912. Office of Publication, 114 Altgeld Hall, Urbana, Illinois 61801.

ABSTRACT

THE CRACKING OF CONCRETE IN HIGHWAY PAVEMENTS AND STRUCTURES IS UNDESIRABLE SINCE CRACKING OF THE CONCRETE IS ASSOCIATED WITH THE DETERIORATION OF BOTH THE CONCRETE AND REINFORCING STEEL. MANY STUDIES ON THE PHENOMENON OF CRACKING IN PLAIN AND REINFORCED CONCRETE HAVE BEEN CONDUCTED; HOWEVER, THESE INVESTIGATIONS HAVE CORRELATED THE CRACKING OF CONCRETE WITH VARIOUS PARAMETERS OF THE CONCRETE AND THE ENVIRONMENT, BUT HAVE NOT CONSIDERED THE MECHANISM OF CRACKING.

A THREE-PHASE INVESTIGATION WAS UNDERTAKEN TO PROVIDE A BETTER UNDERSTANDING OF THE INITIATION AND GROWTH OF CRACKS IN CONCRETE, WHICH IS ESSENTIAL IF CRACKING OF CONCRETE STRUCTURES IS TO BE CONTROLLED. THE EFFECT OF SEVERAL CONCRETE PARAMETERS ON THE FRACTURE TOUGHNESS (MATERIAL'S RESISTANCE TO PROPAGATION OF AN EXISTING FLAW) IS PRESENTED. A SYSTEMS-TYPE ANALYSIS IS PRESENTED TO DESCRIBE THE COMPLEX CRACKING MECHANISM IN CONCRETE STRUCTURES, AND MODELS ARE DEVELOPED FOR STUDYING CRACKING IN CONCRETE BEAMS AND RIGID PAVEMENTS. AN APPROXIMATE SOLUTION FOR THE PROBLEM OF SHRINKAGE STRESSES IN PLAIN AND REINFORCED CONCRETE MEMBERS WHICH ARE EXTERNALLY LOADED IS DEVELOPED.

This page is intentionally blank.

ACKNOWLEDGMENTS

This study was conducted as a part of the research under the Illinois Cooperative Highway Research Program Project IHR-92, "The Control of Cracking of Concrete." The project has been undertaken by the Engineering Experiment Station of the University of Illinois in cooperation with the Illinois Division of Highways of the State of Illinois and the U.S. Department of Transportation, Federal Highway Administration, Bureau of Public Roads.

On the part of the University, the work covered by this report was carried out under the general administrative supervision of D. C. Drucker, Dean of the College of Engineering, R. J. Martin, Director of the Engineering Experiment Station, T. J. Dolan, Head of the Department of Theoretical and Applied Mechanics, and Ellis Danner, Director of the Illinois Cooperative Highway Research Program and Professor of Civil Engineering.

On the part of the Illinois Division of Highways, the work was under the administrative direction of R. H. Golterman, Chief Highway Engineer, and J. E. Burke, Engineer of Research and Development.

Technical advice was provided by a Project Advisory Committee consisting of the following personnel:

Representing the Illinois Division of Highways:

J. E. Burke, Engineer of Research and Development

R. L. Duncan, Field Engineer

W. Griffin, Structural Design Engineer

Representing the University of Illinois:

J. L. Lott, formerly Assistant Professor of Theoretical and Applied Mechanics

G. M. Sinclair, Professor of Theoretical and Applied Mechanics

C. E. Kesler, Professor of Theoretical and Applied Mechanics and of Civil Engineering and David Raecke, Research Associate in the Department of Theoretical and Applied Mechanics, served as Chairman and Secretary, respectively, of the Project Advisory Committee.

CONTENTS

This page is intentionally blank.

FIGURES

This page is intentionally blank.

I. INTRODUCTION

1.1 GENERAL

Undesirable cracking of concrete in highway pavements and structures is associated with the deterioration of both the concrete and the reinforcing steel. Corrective maintenance is costly and inconvenient so that ideal designs should minimize the size of cracks in hardened concrete. Such a control can be improved through a basic understanding of crack development in concrete.

Many studies of cracking in plain and reinforced concrete have been conducted. However, these investigations have correlated the cracking of concrete with various parameters without considering how cracking occurs.

1.2 OBJECT

The object of this investigation is to determine the effect of concrete parameters (mix design) on the cracking of concrete, to study the complex cracking mechanism in concrete structures, and to develop an analytical solution for the problem of volume-change stresses for plain and reinforced concrete. The result, a better understanding of the initiation and growth of cracks in concrete, is essential to control cracking concrete structures.

*Fracture toughness is the material's resistance to propagation of an existing flaw.

1.3 SCOPE

1.3.1 Effect of Concrete Parameters on Fracture Toughness

The fracture toughnesses* of several pastes, mortars, and concretes were determined by flexural tests of specimens containing flaws of various depths cast at the center of the tensile surface. Variables in the tests were: water-cement ratio, air content, degree of hydration, sand-cement ratio, gravel-cement ratio, and gradation and type of coarse aggregate.

1.3.2 Crack Mechanism for Concrete Structures

A systems-type analysis was used to describe the complex cracking mechanism that occurs in concrete structures. The cracking mechanism in a reinforced beam subjected to a pure moment, and the cracking mechanism in a reinforced concrete member with the steel loaded in tension was examined by this approach.

1.3.3 Analytical Study of Crack Development Associated with Volume Change

An approximate solution for the problem of shrinkage stresses in plain and reinforced concrete was developed using finite element analysis. The method can be used to calculate stresses in members which are externally loaded.

Cracking is incorporated into the analysis, and crack width and spacing can be calculated.

1.4 NOTATION

A_s = area of steel reinforcement

a = crack length of an edge-cracked specimen or half the crack length of a center-cracked specimen

a_1, a_2 = constants relating the volume change strains at any point in the element to the y-coordinate of the point

a' = crack length from level of reinforcement to the crack tip

B = flexure specimen width

b = height of an element

$[C]$ = matrix relating stresses to strains

C_1', C_2' = coefficients for different crack lengths

c = cement content of a particular mix, by weight

$c_1,\ldots,c_8$ = constants relating the displacements of a point in an element to the coordinates of that point

$[D]$ = a matrix relating strains to displacements

d = length of an element

d_e = effective depth of reinforced concrete tension member

E_c = effective modulus of elasticity of the concrete

$[F]$ = a column matrix representing the forces at the nodal points of one element

$[\underline{F}]$ = a column matrix representing forces at all nodes

F_b = bond forces

F_i = a force at a point i in the element

$[F_s]$ = a column matrix representing the nodal forces in an element resulting from volume change

G_c = critical energy-release rate at the onset of rapid, unstable crack propagation

h = depth of pavement

K = stress intensity factor at the tip of a flaw

ΔK = change in stress intensity factor due to a load cycle

K' = effective stress intensity factor in the matrix of a heterogeneous material that is assumed to be homogeneous

$[K]$ = symmetrical stiffness matrix for one element

$[\underline{K}]$ = symmetrical stiffness matrix for the entire model

K_c = critical stress intensity factor at the onset of rapid, unstable crack propagation

K_c' = effective fracture toughness

$\bar{K}_c'$ = average effective fracture toughness for a test series

K_{F_b} = stress intensity factor for the concrete subjected only to the resultant forces at the level of the steel

K_{Mc} = stress intensity factor for the concrete subjected only to moments M_c

K_P = stress intensity factor for the concrete subjected only to the axial force P

K_r = stress intensity factor resulting from a series of forces and/or moments

ℓ = shear span

ℓ_s = length of reinforced concrete tension member

ℓ_u = unbonded length of steel reinforcement in concrete tension member

M = applied bending moment

M_c = moments applied to a reinforced concrete beam

n = total number of nodes in the model

P = applied load

r,θ = polar coordinates

s = one-half distance over which concrete is examined in reinforced concrete beam subjected to constant moment

T = force transmitted across cracked section in tension member for equilibrium conditions

T_c = force which concrete transmits across the cracked section in reinforced concrete tension member

T_s = force in steel at cracked section in concrete tension member

t = thickness of reinforced concrete tension member

$[u]$ = column matrix representing the displacements at the four nodes of an element

$[\underline{u}]$ = a column matrix of displacements at all nodes

u_x = x-displacement of a point in the element

u_y = y-displacement of a point in the element

W = flexure specimen depth

w = water content of a particular mix, by weight

x, y = cartesian coordinate system of axes with origin at lower left-hand node of an element

γ_{xy} = shear strain in an element

γ_{xys} = shear volume change strain in an element

Δ = crack opening displacement at level of reinforcement

$[\varepsilon]$ = a column matrix representing the strains in an element

ε_i^T = transpose of matrix of compatible strains due to a unit displacement in the direction of F_i

ε_x = normal strain in x-direction in an element

ε_y = normal strain in y-direction in an element

ε_{xs} = normal volume change strain in the x-direction

ε_{ys} = normal volume change strain in the y-direction

η = nondimensionalized coordinate y/b

ζ = nondimensionalized coordinate x/d

$[\sigma]$ = a column matrix representing the stresses in an element

$[\sigma_s]$ = a matrix representing volume change stresses

σ_x = stress normal to y-z plane in x-direction

σ_y = stress normal to x-z plane in y-direction

τ_{xy} = shear stress on plane perpendicular to x-axis in y-direction

II. EFFECT OF CONCRETE PARAMETERS ON FRACTURE TOUGHNESS

2.1 INTRODUCTION

2.1.1 Linear-Elastic Fracture Mechanics

Linear-elastic fracture mechanics is a study of the stress and displacement fields near the tip of a flaw in an ideal, homogeneous, elastic material at the onset of rapid, unstable crack propagation, i.e., fracture. Its concepts are most applicable to brittle materials in which the inelastic region near the crack tip is small compared to flaw and specimen dimensions so that elastic stress field equations provide a good approximation[1]:*

$$\sigma_x = \frac{K}{\sqrt{2\pi r}} \cos\frac{\theta}{2}\left[1-\sin\frac{\theta}{2}\sin\frac{3\theta}{2}\right],$$

$$\sigma_y = \frac{K}{\sqrt{2\pi r}} \cos\frac{\theta}{2}\left[1+\sin\frac{\theta}{2}\sin\frac{3\theta}{2}\right], \quad (1)$$

$$\tau_{xy} = \frac{K}{\sqrt{2\pi r}} \sin\frac{\theta}{2}\cos\frac{\theta}{2}\cos\frac{3\theta}{2},$$

where r and θ are polar coordinates with origin at the crack tip.

Equation (1) indicates that the stress and displacement fields can be expressed in terms of a stress intensity factor K which is a function of loading and crack geometry. The evaluation of K at the onset of rapid, unstable crack propagation yields the critical stress intensity K_c which is assumed to be a material property called the fracture toughness, i.e., the material's resistance to propagation of an existing flaw. Fracture can thus be predicted for a structure since crack propagation will occur when the stress intensity factor reaches its limiting condition K_c.

As the ratio of plastic zone size to specimen dimensions increases, the inelastic region becomes significant and adjustments must be made to correct for effects of plastic strains adjacent to the crack tip region.[2] An exact solution to correct for the zone of yielding is presently unknown; however, an approximate solution can be attained by assuming a crack tip extension to the central portion of the inelastic region and solving the problem with elastic stress field equations for the increased crack length.

2.1.2 Applications of Fracture Mechanics to Concrete

Several applications of linear-elastic fracture mechanics have been made to pastes, mortars, and concretes.[3-7] Concrete, a polyphase material, has a more complex fracture process than a homogeneous, ideally brittle material. Fracture of the concrete can occur by

*Superscript numbers in parentheses refer to entries in References, Chapter VII.

fracture of the cement paste, fracture of the aggregate, failure of the bond between the cement paste and aggregate, or any combination of these mechanisms.

Kaplan[3] was the first to apply fracture mechanics to concrete when he investigated one mortar and two concretes. An analytical and experimental approach, both neglecting slow crack propagation prior to fracture, were used to evaluate the critical strain energy release rate G_c. The results obtained by Kaplan indicated that G_c was influenced by the mix proportions, specimen dimensions, and loading.

Lott and Kesler[6] conducted a study to develop a hypothesis for propagation of cracks in plain concrete and to compare the hypothesis to results of an experimental investigation of crack propagation in several mortars and concretes. It was suggested that the critical stress intensity factor K_c for plain concrete was derived from the stress intensity factor of the paste and a crack arresting mechanism developed by the heterogeneity of the concrete. Since the critical stress intensity factor for the paste was a material constant, variations in the critical stress intensity factor of the concrete were reflected through the arresting function. The effects of several concrete parameters (water-cement ratio, sand-cement ratio, and gravel-cement ratio) on the fracture toughness of the concrete were evaluated.

For the range of variables investigated, it was found that: the critical stress intensity factor was independent of water-cement ratio for the three mortars and for various concretes where the aggregate percentages remained constant; the critical stress intensity factor was independent of fine aggregate percentage for three mortars with the same water-cement ratio; the critical stress intensity factor varied directly with coarse aggregate content for concretes with the same water-cement ratio and fine aggregate content; and the critical stress intensity factor for concrete was found to be approximately 20 per cent greater than that for a mortar with the same water-cement ratio and fine aggregate content.

2.2 EXPERIMENTAL INVESTIGATION

2.2.1 General

The fracture toughnesses of several pastes, mortars, and concretes were determined by flexural tests of specimens containing flaws of various depths cast at the center of the tensile surface.[7] Parameters investigated included: water-cement ratio, air content, degree of hydration, sand-cement ratio, gravel-cement ratio, and gradation and type of coarse aggregate.

2.2.2 Materials

Type I portland cement was used in all mixes. The fine aggregate used was a Wabash River sand from near Covington, Indiana. Two gravels were used in the concrete series: a Wabash River gravel from near Covington, Indiana, and a crushed limestone which was obtained locally.

The air-entraining agent used was a proprietary compound consisting of an aqueous solution of salts of sulfonated hydrocarbons containing a catalyst.

2.2.3 Specimen Description

Nominal dimensions of the paste and mortar flexural specimens were 2 by 2 by 14 in., and nominal dimensions of the concrete specimens were 4 by 4 by 12 in. A flaw was cast at the center of the tensile surface of the specimens. The flaw was formed with a 0.003-in.-thick piece of teflon-coated fiberglass cloth. Nominal flaw depths were: 0.25 in., 0.5 in., and 1.0 in. for the paste and mortar specimens, and 0.5 in., 1.0 in., and 1.5 in. for the concrete specimens. Actual dimensions of the flexure specimens were measured after testing since variations in nominal dimensions occurred in fabrication.

2.2.4 Fabrication and Curing

A two-cubic-foot horizontal pan mixer was used. The dry ingredients were blended one minute before water was added to the mix. After addition of the water, the mixing was continued for three minutes. When air-entraining agents were used, they were added to the mix water.

The flexure specimens were cast with the plane of the flaw in a vertical position. The molds were filled in one lift and compacted on a vibrating table. A total of twenty flexural specimens were cast in steel forms for each series of the paste and mortar series, and a total of eight flexural specimens were cast in plywood forms for each series of the concrete series. The exposed surface of all specimens was troweled smooth immediately after casting.

Two to four hours after casting the specimens were covered with wet burlap and plastic sheeting to prevent the loss of moisture. Approximately twenty-four hours after casting, the specimens were demolded and stored in a moisture room for curing at 100 per cent relative humidity. The specimens were removed from the moisture room at various ages and stored in water until they were tested.

2.2.5 Testing Procedure

A hydraulic testing machine was used for the flexural tests. Figure 1 shows the test setup. The lower loading plate acted as a dynamometer to measure load applied to the specimen. A deformeter, supported by needlepoint screws, was used to measure elongation of the tensile surface.

Prior to each series of flexural tests, the deformeter and dynamometer were calibrated. After calibration, the deformeter was placed between the needlepoint screws of the first specimen and precompressed to a pseudozero point. The recorder was zeroed and load was applied at a rate of approximately 250 lb per minute for the paste and mortar specimens and 1500 lb per minute for the concrete specimens until failure occurred.

2.3 EXPERIMENTAL RESULTS

2.3.1 Load-Deformation Curves

During each test, a recorder plotted a continuous record of deformation response against load response until failure of the flexural specimen. Typical load-deformation curves for a concrete series are presented in Figure 2.

2.3.2 Stress Intensity Factor

Brown and Srawley[8] used boundary value collocation calibrations to develop the following expression for the stress intensity factor K for a single-

edge-cracked specimen subjected to pure bending:

$$K = Y \frac{6Ma^{\frac{1}{2}}}{BW^2} \qquad (2)$$

where

$$Y = 1.99 - 2.47\,(a/W) + 12.97\,(a/W)^2 - 23.17\,(a/W)^3 + 24.80\,(a/W)^4 ,$$

$$M = \frac{P\ell}{2} ,$$

and a is the flaw depth, W is the specimen depth, P is the applied load, ℓ is the shear span, and B is the specimen width.

In the evaluation of K_c using Equation (2), it was assumed that the material was homogeneous and the flaw depth at failure was equal to the cast flaw depth. Since concrete is heterogeneous and the stress intensity factor is a function of the instantaneous crack depth, the analysis yields an effective stress intensity factor K' rather than the actual stress intensity factor.

The effective fracture roughness K_c', a measure of concrete's resistance to propagation of an existing crack, is the determination of K at M_{max} from Equation (2). Figure 3 presents K_c' and P_{max} as a function of a/W for a concrete series. The horizontal line in Figure 3 represents the mean value of effective fracture toughness for the particular test series, $\bar{K}_c'$.

2.3.3 Effect of Concrete Parameters on Effective Fracture Toughness

Water-Cement Ratio

In the paste series there was a decrease in $\bar{K}_c'$ of 43.3 per cent when the water-cement ratio was increased from 0.27 to 0.36, while in the mortar series $\bar{K}_c'$ decreased 18.3 per cent when the water-cement ratio was increased from 0.45 to 0.60 as shown in Figure 4. However, in the concrete series $\bar{K}_c'$ was independent of the water-cement ratio for the range of water-cement ratios investigated as shown in Figure 4.

Air Content

In the paste series there was a 23.4 per cent decrease in $\bar{K}_c'$ when the air content was increased from 2.0 to 8.0 per cent as shown in Figure 5. In the mortar series $\bar{K}_c'$ decreased by 19.2 per cent when the air content was increased from 3.0 to 9.0 per cent as shown in Figure 5. $\bar{K}_c'$ decreased by 8.2 per cent when the air content in the concrete series was increased from 2.0 per cent to 12.0 per cent as shown in Figure 5.

Curing Time

For 28 days moist cure $\bar{K}_c'$ was 6.5 per cent greater than $\bar{K}_c'$ for six days moist cure as shown in Figure 6 for the paste series. For the mortar series there was a 47.5 per cent increase in $\bar{K}_c'$ when the length of moist cure was increased from three days to 92 days as shown in Figure 6. When the length of moist cure was increased from three days to 28 days for concrete using a river gravel coarse aggregate, $\bar{K}_c'$ increased 54.2 per cent. However, the increase in $\bar{K}_c'$ was only 7.7 per cent when the length of moist cure was increased from 28 days to 90 days as shown in Figure 7. When a crushed limestone coarse aggregate was used, $\bar{K}_c'$ increased 23.0 per cent with an increase in moist cure from three days to 28 days; however, there was no apparent change in $\bar{K}_c'$ when

the length of moist cure was increased from 28 days to 90 days as shown in Figure 7. The percentage increases in $\bar{K}_c'$ when the moist curing period was increased from six days to 28 days for the paste series, the mortar series, the concrete series cast with a crushed limestone coarse aggregate, and the concrete series cast with a river gravel coarse aggregate were 6.5 per cent, 12.4 per cent, 21.3 per cent and 24.2 per cent, respectively.

Fine Aggregate Content

In the mortar series there was a 16.2 per cent increase in $\bar{K}_c'$ when the fine aggregate content was increased from 55.0 per cent to 70.0 per cent as shown in Figure 8. However, for the concrete series there was a 2.3 per cent decrease in $\bar{K}_c'$ when the fine aggregate content was increased from 35.0 per cent to 50.0 per cent as shown in Figure 9.

Gravel Content, Gradation, and Type

For the concretes cast with crushed limestone coarse aggregate, $\bar{K}_c'$ increased 13.3 per cent when the fineness modulus was increased from 6.3 to 7.1 as shown in Figure 10. When the percentage of coarse aggregate was increased from 0.0 per cent to 50.0 per cent there was a 37.0 per cent increase in $\bar{K}_c'$ as shown in Figure 11.

For the concrete series cast with a crushed limestone $\bar{K}_c'$ was 28.9 per cent, 17.7 per cent, and 1.7 per cent higher than $\bar{K}_c'$ for the concrete series cast with a river gravel coarse aggregate at ages of three days, six days and 28 days, respectively. However, at an age of 90 days, $\bar{K}_c'$ for the concrete series cast with a river gravel coarse aggregate was 5.0 per cent higher than the concrete series cast with a crushed limestone coarse aggregate as shown in Figure 7.

2.4 DISCUSSION OF RESULTS

2.4.1 Behavior of Fracture Toughness Specimens

The load-deformation curves (Figure 2) illustrate the stages of behavior of the concrete near the tip of the flaw: linear stage where the cement paste matrix has no crack extension; slow cracking stage in which stable cracking occurs to result in a decreasing slope of the load-deformation curve; and fracture stage where unstable crack propagation occurs and results in the deformation increasing without an increase in applied load.

2.4.2 Effect of Concrete Parameters on $\bar{K}_c'$

Water-Cement Ratio

There was a decrease in the effective fracture toughness of the paste and mortar series with increasing water-cement ratio because the fracture toughness was dependent on the strength of the cement paste matrix which was a function of gel-space ratio.[9] With increasing water contents the gel-space ratio decreased resulting in a reduction of strength and effective fracture toughness. The fine aggregate of the mortar series reduced the effect of the water-cement ratio because of the crack arresting phenomenon of the fine aggregate particles.[6]

The effective fracture toughness of concrete depended on both the fracture toughness of the paste and the

presence of coarse aggregate. The range of water-cement ratios apparently did not affect the effective fracture toughness of the concrete because the effect of the aggregate as a crack arresting function was more significant than the effect of the water-cement ratio on the paste matrix strength.

Air Content

Increasing the air content of the matrix resulted in a decrease in effective fracture toughness because of a reduced matrix strength. With increasing aggregate contents, the decrease was not as significant because of the crack arresting phenomenon of the aggregate.

Curing Time

The increase in effective fracture toughness with age was the result of continuing hydration of the cement particles to produce a higher strength.

Fine Aggregate Content

The effective fracture toughness for the mortar increased with an increasing amount of fine aggregate because of an increased concentration of crack arresting particles in the matrix. The effective fracture toughness of the concrete was not significantly affected by an increasing fine aggregate content because the coarse aggregate particles were much better crack arresters and thus concealed the effect of the fine aggregate.

Gravel Content, Gradation and Type

The effective fracture toughness increased with an increase in maximum size particles because the larger aggregate particles are more effective as crack arresters. However, a maximum size can be reached in conjunction with a poor gradation that will produce a lower effective fracture toughness because of the effects of segregation as shown in Figure 10 for a fineness modulus of 7.45.

An increased gravel content increased the effective fracture toughness because the larger gravel content enlarged the concentration of crack arresters in the matrix.

The effective fracture toughness for the crushed limestone coarse aggregate was greater than the effective fracture toughness for the river gravel coarse aggregate until 28 days, indicating that the crushed limestone apparently developed greater bond strength. However, after an age of 28 days the bond strengths for the two types of coarse aggregate appeared to be equivalent.

III. CRACK MECHANISM FOR CONCRETE STRUCTURES

3.1 INTRODUCTION

Control of cracking in concrete structures subjected to varying load and environment requires a basic understanding of the crack mechanism to correlate laboratory data with service conditions. The fracture process in concrete structures is similar to the fracture that occurs in the fracture toughness specimens of Chapter II, in that both crack growths are associated with a fracture phenomenon that occurs in the highly stressed region surrounding the crack tip. In the fracture toughness specimen, the crack propagates when the stress intensity factor of Equation (2) reaches the effective fracture toughness K_c'. There is no simple stress intensity factor for a crack in a concrete structure since the structural components interact with each other and with the stress field surrounding the crack tip. A systems-type analysis of the fracture process is used to describe the complex cracking mechanism for concrete structures.

3.2 FRACTURE SYSTEM

Hahn and Rosenfield[10] have presented a systems-type analysis of the fracture problem and applied it to the fracture of metal plates and incorporated the effect of yielding in the region of the crack tip. A fracture system of processes that responds to outside stimuli and interacts with each other was developed. Quantitative analysis of the system requires that the stimuli and responses of the various processes be expressed in compatible terms (stress), which can be either theoretical or empirical.

A similar system is useful for analysis of cracking of concrete structures and is shown in Figure 12. The structure[1] consists of the structural elements such as concrete, reinforcement, and supports, including pavement base materials. The relation between load, environment, and the stresses in the various structural elements is required. Stress-strain modifiers[11] include flaws, cracks, inclusions, and other stress concentrators. The general level of stress is intensified locally near these modifiers. The linear-elastic fracture mechanics techniques are used to evaluate the elastic stress field surrounding sharp flaws. Inelastic deformations (III) may occur in regions that are highly stressed relative to strength. These inelastic deformations modify the relative stiffness of the structural elements and cause a redistribution of stress in the structure. Cracking mechanisms (IV) are initiated when critical conditions develop in the region of a crack tip,

and crack growth takes place. This crack growth also modifies the relative stiffness of the structural elements and results in a stress redistribution.

The general fracture process of a concrete structure is as follows:

The input (A) of load and environment to the structure (I) causes stresses to develop within the structural elements. The general stress levels are transmitted (B) to any modifiers (II) in the system. The stresses are increased and transmitted (D) to the inelastic deformations (III) and transmitted (F) to the fracture mechanisms (IV). At a critical stress level the inelastic deformations occur and are transmitted back (E) to the modifiers, and at some critical condition existing cracks propagate, and the effect of increased crack lengths are fed back (G) to the modifiers. These effects on the modifiers are reflected back (C) to the structure as changes in relative stiffness and result in stress redistribution.

Inelastic deformations tend to increase the relative stiffness of concrete and promote cracking, while crack growth tends to reduce the relative stiffness of the concrete and arrests crack growth.

The systems-type analysis of cracking concrete structures is based on a free body diagram of the concrete portion of the structure, which is the structural element that contains the crack that will propagate. The effects of load, environment, reinforcement, and other structural elements on concrete fracture are obtained by superposition. The stress intensity factor describing the stress field surrounding the tip of the crack in the concrete is evaluated separately for each action on the free body. The resultant stress field is obtained by summing the individual stress intensity factors K_i, and the condition of crack instability occurs when the resultant K_r equals the effective fracture toughness of the concrete K_c'.

$$\sum_{i=1}^{i=m} K_i = K_r \leq K_c' \qquad (3)$$

3.3 FRACTURE OF CONCRETE STRUCTURES

The analysis of concrete cracking in structures is based on a resultant stress intensity factor for a crack in the concrete, which is the stress modifier associated with the cracking mechanism that interacts with the loads and the other elements of the structure. A concrete body containing the crack is isolated, and the stress intensity factors for the various actions are determined using available expressions and summed to obtain the resultant stress intensity factor K_r. Equilibrium crack conditions, which relate crack geometry and load, correspond to the limiting condition of Equation (3),

$$K_r = K_c. \qquad (3\text{-}1)$$

3.3.1 Crack in Constant Moment Region of Reinforced Concrete Beam

The cracking mechanism in a reinforced concrete beam subjected to a constant moment M is analyzed by considering the concrete within a distance s of the crack as shown in Figure 13. The concrete is subjected to moments M_c and axial compressive forces P which are the actions of the adjacent concrete, and of resultant bond forces F_b at the level of the reinforcement, which are

the net forces transferred to the concrete over the interval s. The resultant stress intensity factor K_r which describes the stress field surrounding the crack tip in the beam is

$$K_r = K_{Mc} + K_P + K_{F_b} \qquad (4)$$

where K_{Mc} is the stress intensity factor for the concrete subjected only to the moments M_c, K_P is the stress intensity factor for the concrete subjected only to the axial forces P, and K_{F_b} is the stress intensity factor for the concrete subjected only to the resultant forces at the level of the steel. Expressions for these stress intensity factors are available.[11,12] However, the magnitudes of M_c, P, and F_b are functions of the forces in the reinforcement. The steel forces are dependent upon the inelastic deformations associated with unbonding and cannot be defined with sufficient accuracy for a quantitative analysis of cracking.

A qualitative analysis of cracking indicates that K_{Mc} is the parameter that tends to cause crack extension; K_P is negative for compressive forces and tends to arrest crack growth; K_{F_b} is negative when the bond forces F_b act toward the crack and tends to arrest cracking and is positive and tends to cause cracking when the load forces act away from the cracks.

3.3.2 Crack in Reinforced Concrete Tension Member

A reinforced concrete member with the steel loaded in tension, Figure 14, has been suggested as a useful model of the cracking mechanism in beams,[13] and crack development under increasing load has been investigated.[14] A quantitative analysis of crack equilibrium is based on the concrete element of Figure 15. The only forces acting on the concrete are the bond forces F_b that develop as the reinforcement elongates. The unbonding at the free ends and at the cracked section affect the magnitude of the bond forces. The bond forces cause an opening Δ of the crack at the level of the reinforcement.

The stress intensity factor K may be expressed in terms of the bond forces F_b or the opening Δ.[12]

$$K = \frac{C_1' F_b}{t\, d_e^{\frac{1}{2}}} = \frac{C_2' E_c}{d_e^{\frac{1}{2}}}\, \Delta \qquad (5)$$

where t is the thickness, d_e is the effective depth, E_c is the modulus of elasticity of the concrete, and C_1' and C_2' are coefficients that are evaluated for various crack lengths a', effective depths d_e, and specimen lengths ℓ_s.[12]

The maximum equilibrium crack length corresponds to a stress intensity factor K that is equal to the effective fracture toughness of the concrete K_c',

$$K = K_c' \,. \qquad (6)$$

The force which the concrete transmits across the cracked section, T_c, is equal to the bond force F_b,

$$T_c = F_b = \frac{K_c'\, t\, d_e^{\frac{1}{2}}}{C_1'} \,, \qquad (7)$$

and is usually small relative to the force in the steel T_s. The wedge opening Δ which corresponds to an equilibrium crack is

$$\Delta = \frac{K_c'\, d_e^{\frac{1}{2}}}{C_2'\, E_c} \qquad (8)$$

and is assumed to be equal to the elongation of the steel reinforcement over an equivalent unbonded length ℓ_u, and

$$\Delta = \frac{T_s \ell_u}{A_s E_s} \qquad (9)$$

where T_s is the force in the steel at the cracked section, A_s is the steel area, and E_s is the modulus of elasticity for steel. The total force T transmitted across the cracked section for equilibrium conditions is

$$T = T_c + T_s = \frac{K_c' t d_e^{\frac{1}{2}}}{C_1'} + \frac{K_c A_s E_s d_e^{\frac{1}{2}}}{C_2' \ell_u E_c} . \qquad (10)$$

T_c is unique for a given equilibrium crack length, and T_s varies inversely with the unbonded length ℓ_u. The total load T may be calculated for a given crack length a' by substituting various unbonded lengths ℓ_u into Equation (10). This has been done for the specimen geometry and material properties of crack specimens of Reference (14), and the relationships between T and the ratio of crack length to effective a'/d_e, are given in Figure 16 for different unbonded lengths. The effective fracture toughness has been assumed to be approximately 0.6 ksi$\sqrt{\text{in}}$.

The relationships of Figure 16 indicate the following:

(a) The equilibrium crack lengths a' increase with total force T if the unbonded length ℓ_u is constant;

(b) The total force T transmitted across a given cracked section decreases as the unbonded length increases;

(c) An increased unbonded length is associated with an increased crack length corresponding to a virtual load increase.

Crack data from Reference (14) is shown in Figure 16 for increasing loads. The first cracks initiated in two different specimens at the 20 kip load level. They corresponded to equivalent unbonded lengths of 0.5 and 1.2 in. At the higher load levels of 25 and 35 kips, the crack lengths corresponded to unbonded lengths of 1.2 to 1.5 in. At crack initiation there was a large range in the unbonded length. As the load increased, the unbonded lengths increased and the range was reduced. This is an example of the interaction of an inelastic deformation, the unbonding, with the concrete cracking mechanism.

3.3.3 Crack in Rigid Pavement

Cracking in rigid pavements may be analyzed by using the cracked beam on an elastic foundation of Figure 17. The stress intensity factor should vary with the inverse of crack length

$$K = f\left(\frac{1}{a}\right) , \qquad (11)$$

since an increase in the crack length a transfers more load to the elastic foundation in the region of the crack and reduces the stresses on the cracked section. The limiting condition is a crack through the pavement depth (a = h), and the load is still transferred to the foundation. This is a stable crack growth condition. Crack growth arrests additional cracking until the applied load is increased. Crack growth may also be caused by repeated loadings, and this model should find applications in the fatigue of rigid concrete pavements.

IV. ANALYTICAL STUDY OF CRACK DEVELOPMENT ASSOCIATED WITH VOLUME CHANGE

4.1 INTRODUCTION

The volume of concrete changes with age through shrinkage or swelling associated with moisture movement. Nonuniform volume change of concrete takes place because of nonuniform moisture exchange. Changes occur in the shape of concrete members, and stresses are induced. The nonuniform shrinkage of concrete has not been studied to the same extent as uniform shrinkage, and more information is available in the literature on uniform shrinkage of concrete than on nonuniform or relative shrinkage of concrete.

Theoretical analysis of shrinkage stresses in concrete involves a tedious solution of partial differential equations of diffusion and compatibility. If the analysis of reinforced concrete is desired, these differential equations become more complex.

In recent years the solutions to the problems that have been extremely difficult to solve by means of analytical approaches have been obtained by numerical computations through the use of digital computers. In particular, the analysis of shrinkage stresses in plain and reinforced concrete can be performed by use of the finite element method.

4.2 DEVELOPMENT OF STIFFNESS MATRIX FOR FINITE ELEMENT ANALYSIS

4.2.1 Assumptions

The following assumptions are made in developing the finite element model:

(a) Concrete and steel have linear stress-strain diagrams;

(b) Loads and deformations are applied to nodal points;

(c) Shrinkage strains are applied to elements;

(d) A perfect bond exists between steel and concrete;

(e) Concrete and steel are homogeneous and isotropic materials and each has an identical stress-strain relation in tension and compression (except concrete is assumed to fail at a limiting stress in tension but not in compression);

(f) The steel element has no physical dimensions and is assumed to be present on a horizontal line of nodes only;

(g) Loading is one directional.

4.2.2 Concrete Element

Elements of various shapes may be used in the finite element analysis. However, the shape of the element should be selected so it fits the needs of the analysis. In this analysis a rectangular element was selected since it fits

the structural shapes (beams and slabs) in which shrinkage is to be studied. A rectangular element also allows application of linearly varied shrinkage strains to any particular element. Figure 18 depicts a typical rectangular element. The four corners of the rectangle are called the nodes. The forces and displacements that are to be applied to the structural element being analyzed by the finite element method must be applied through these nodal points.

The stresses and strains in any one element are not constants, but depend on the coordinates of the point at which they are evaluated. The coordinates of a point in any one element are measured from a set of axes with the origin at the lower left node of the element as shown in Figure 18.

A set of stresses, σ_x, σ_y, τ_{xy}, is calculated for each node and also for the center of the element. Principal stresses are calculated at the center of the element. In order to detect the occurrence of cracking in an element, the maximum principal stress is compared with the limiting stress at which concrete is assumed to crack.

4.2.3 Steel Element

The physical size of steel is usually small compared to concrete. In particular, when one considers shrinkage reinforcement, this difference in size becomes very noticeable. In this study, the steel element is assumed to have no physical dimension but only mechanical properties. The steel is assumed to be present along a line of horizontal nodal points as shown in Figure 19. No steel is assumed to be present inside the concrete elements. There is no restriction on the position of the horizontal reinforcement other than being restricted to a single line.

4.2.4 Analytical Model

The complete reinforced concrete model used in this study is shown in Figure 19. The model is assumed to be of unit thickness, although this is not a necessary requirement for the analysis.

Boundary conditions specified at the nodal points on the model can be varied to fit a specific problem, i.e., a fixed condition at the left end of the beam is realized when the displacements in the x- and y-directions are set equal to zero for all the nodes at the left-most side of the model. Loads are applied at the nodes, and distributed loads are represented by a series of concentrated loads acting at the nodes. If the model is loaded by inducing deformations on it, the deformations must also be applied at the nodes. Only strains are applied to the elements.

4.2.5 Derivation of Stiffness Matrix for One Element

In this study the finite element problem is restricted to two dimensions resulting in either a plane stress or plane strain condition. The stiffness matrix is derived for the general case partly from the work of Przemieniecki[15] and will be valid for both plane stress and plane strain.

Consider the element in Figure 18. To simplify the analysis, the nondimensionalized coordinates $\xi = x/d$ and $\eta = y/b$ are used.[15] The displacements at any point in an element are functions of the coordinates of the point and will

be assumed to be of the following nature:

$$u_x = C_1\zeta + C_2\zeta\eta + C_3\eta + C_4$$
$$u_y = C_5\zeta + C_6\zeta\eta + C_7\eta + C_8 \qquad (12)$$

where:

u_x, u_y are displacements in the x- and y-directions and C_1, C_2,..., C_8 are constants which can be evaluated from the following boundary conditions:

at (0, 0) $u_x = u_1$, $u_y = u_2$
(0, b) $u_x = u_3$, $u_y = u_4$
(d, b) $u_x = u_5$, $u_y = u_6$
(d, 0) $u_x = u_7$, $u_y = u_8$

The displacements will then be represented by

$$u_x = (1-\zeta)(1-\eta)u_1 + (1-\zeta)\eta u_3 + \zeta\eta u_5 + \zeta(1-\eta)u_7 , \qquad (12a)$$
$$u_y = (1-\zeta)(1-\eta)u_2 + (1-\zeta)\eta u_4 + \zeta\eta u_6 + \zeta(1-\eta)u_8 .$$

The total strains can be determined by differentiating the displacement equations

$$\varepsilon_x = \frac{\partial u_x}{\partial x} = \frac{1}{d}\frac{\partial u_x}{\partial \zeta} ,$$
$$\varepsilon_y = \frac{\partial u_y}{\partial y} = \frac{1}{b}\frac{\partial u_y}{\partial \eta} , \qquad (13)$$
$$\gamma_{xy} = \frac{\partial u_x}{\partial y} + \frac{\partial u_y}{\partial x} = \frac{1}{b}\frac{\partial u_x}{\partial \eta} + \frac{1}{d}\frac{\partial u_y}{\partial \zeta} ,$$

where ε_x and ε_y are the normal strains in the x- and y-directions, respectively, and γ_{xy} is the shear strain.

The strain-displacement relationship for the rectangular element becomes in matrix notation

$$[\varepsilon] = [D][u] \qquad (13a)$$

where [D] is a matrix relating strains to displacements and [u] is a column matrix representing the displacements at the four nodes of an element. It is important to note that the strain in each element is not a constant, but is dependent on the coordinates of the point at which it is to be evaluated.

The stress-strain relationship for the element can be represented in matrix notation as

$$[\sigma] = [C][\varepsilon] \qquad (14)$$

where [C] is a matrix relating stresses to strains and [ε] is a column matrix representing the strains in an element. Substitution of Equation (13a) into Equation (14) yields

$$[\sigma] = [C][D][u] , \qquad (15)$$

which relates the stresses to the nodal displacements for one element.

A typical force F_i at a point i in the element can be calculated by the unit displacement theorem[15]

$$F_i = \int_v \varepsilon_i^T \sigma \, dV \qquad (16)$$

where:

ε_i^T = transpose of matrix of compatible strains due to a unit displacement in the direction of F_i,

σ = stress matrix resulting from all forces acting on the element,

dV = element of volume in the element,

$\int_v$ = integration over total volume of the element.

The forces at the nodal points of the elements can be found by substituting the matrices into Equation (16) and then integrating the product over the total volume of the element.

SUPPORTING DATA

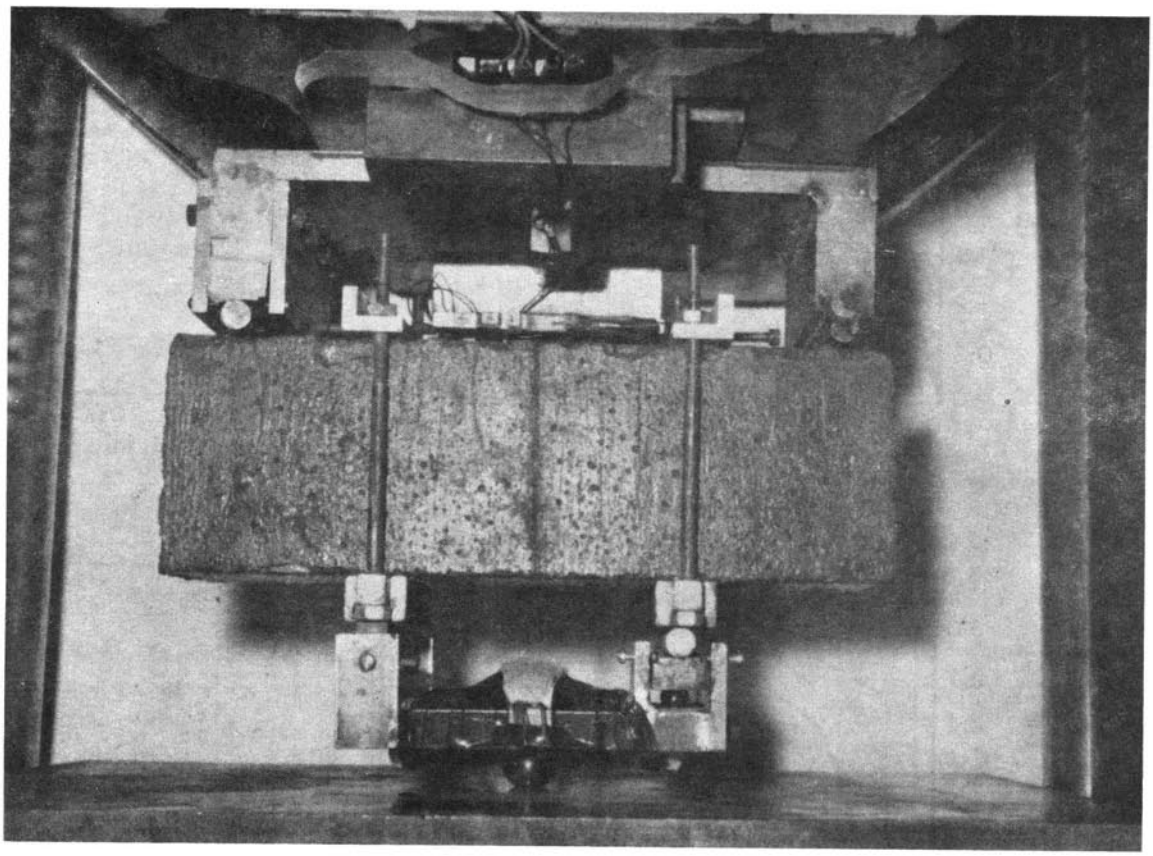

FIGURE 1. TEST SETUP

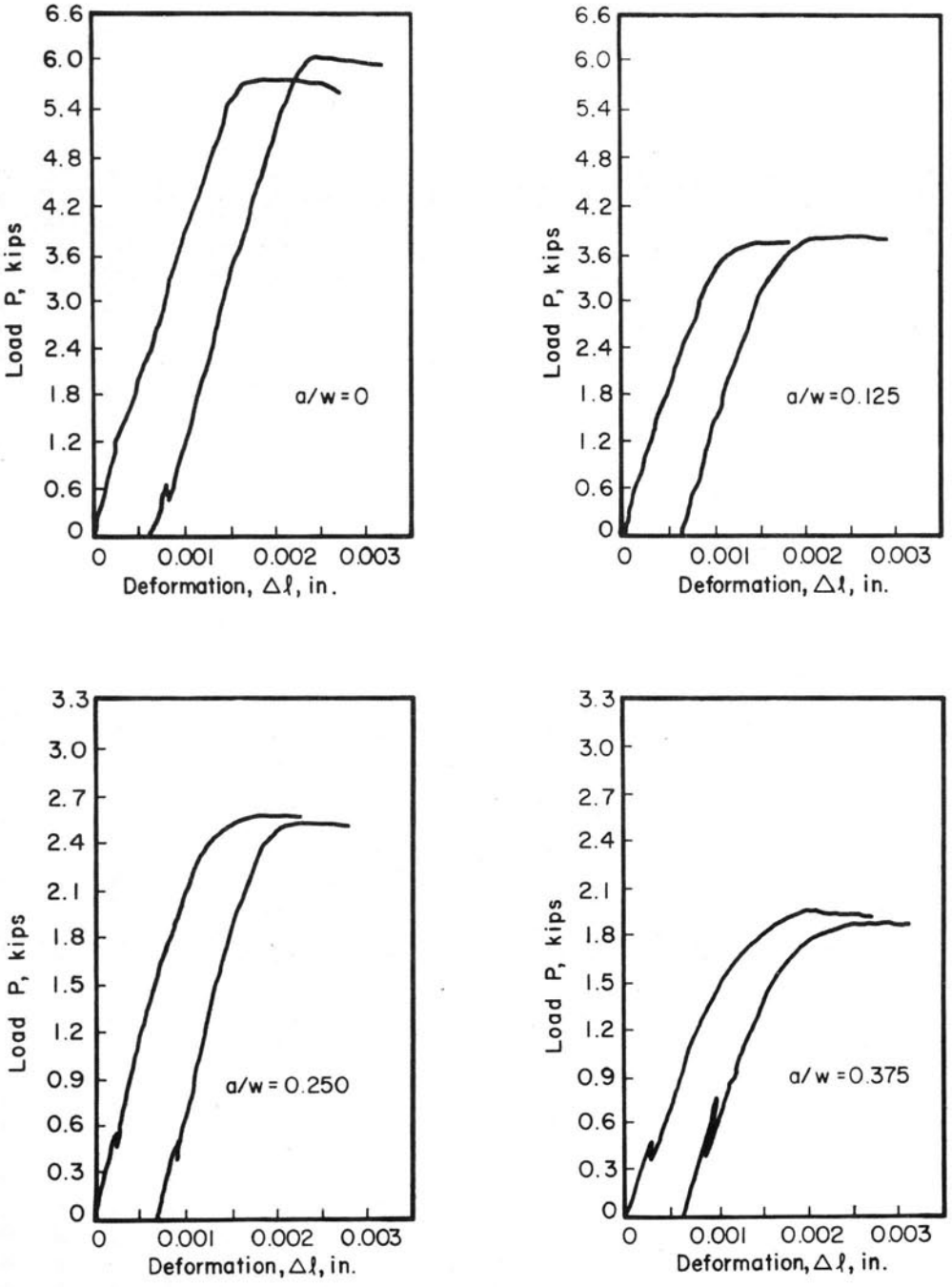

FIGURE 2. TYPICAL LOAD-DEFORMATION CURVES: CONCRETE

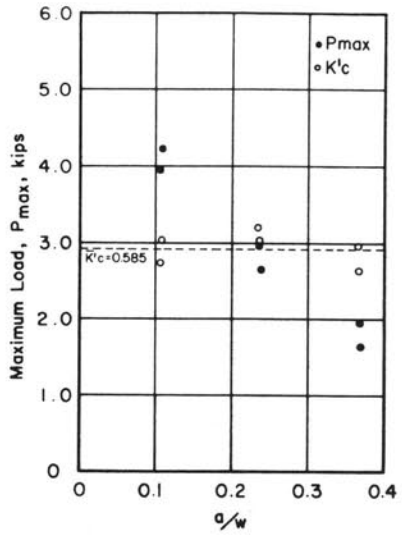

FIGURE 3. MAXIMUM LOAD AND EFFECTIVE FRACTURE TOUGHNESS VS A/W.

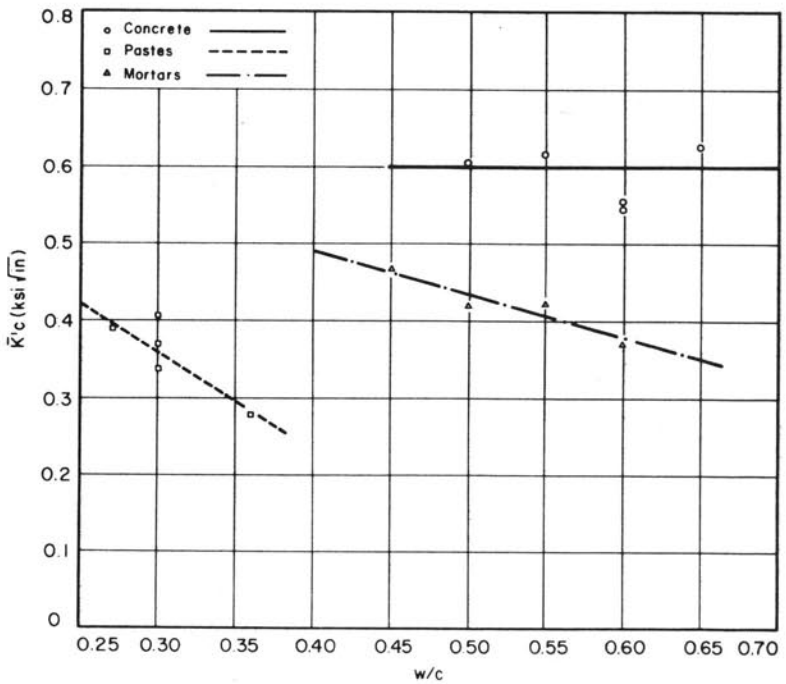

FIGURE 4. EFFECT OF W/C RATIO ON $\bar{K}'_c$

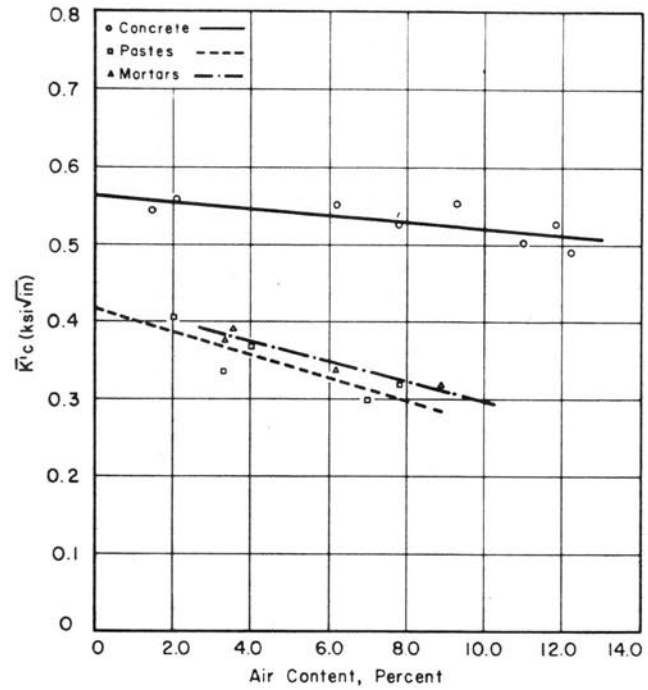

FIGURE 5. EFFECT OF AIR CONTENT ON $\bar{K}'_c$

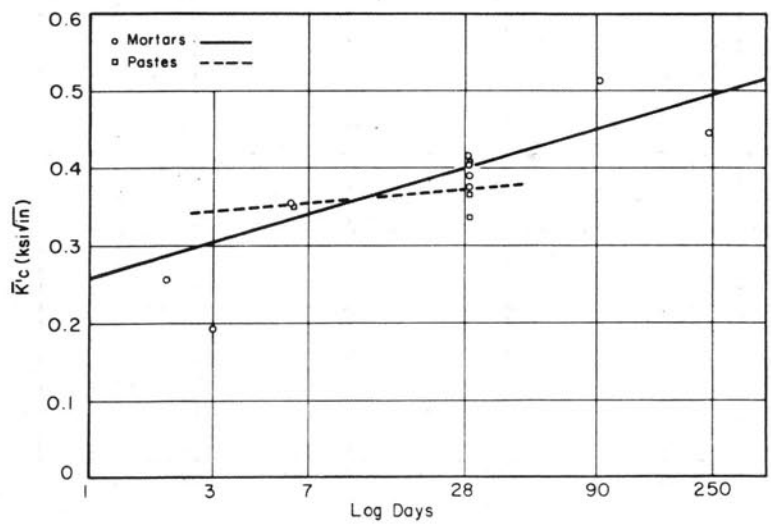

FIGURE 6. EFFECT OF CURING TIME ON $\bar{K}'_c$: MORTARS & PASTES

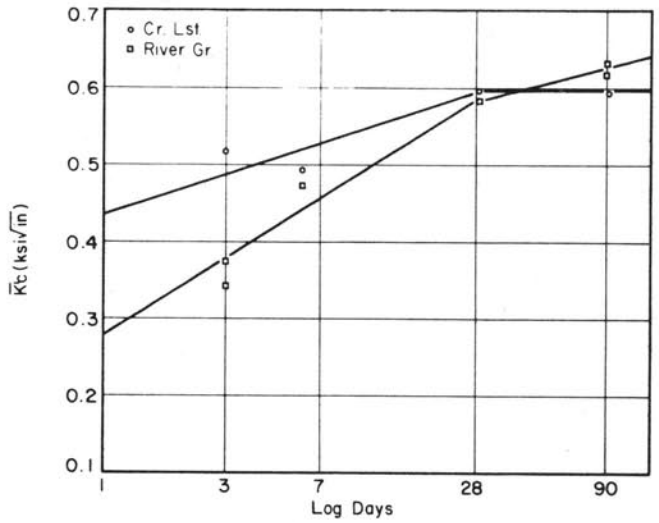

FIGURE 7. EFFECT OF CURING TIME AND TYPE OF COARSE AGGREGATE ON $\bar{K}'_c$: CONCRETES

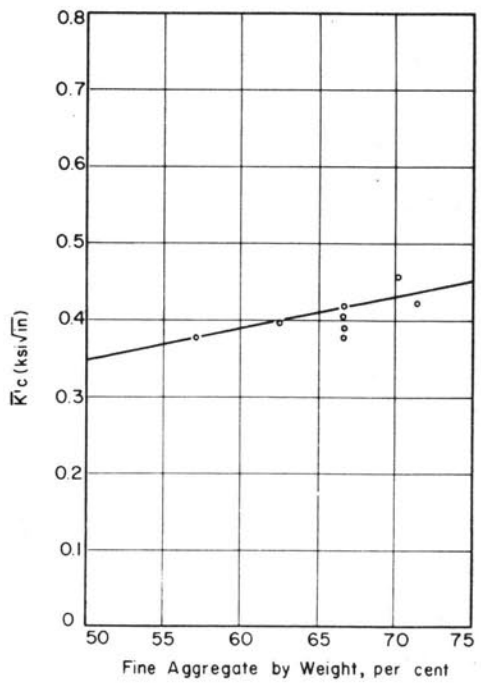

FIGURE 8. EFFECT OF FINE AGGREGATE ON $\bar{K}'_c$: MORTARS

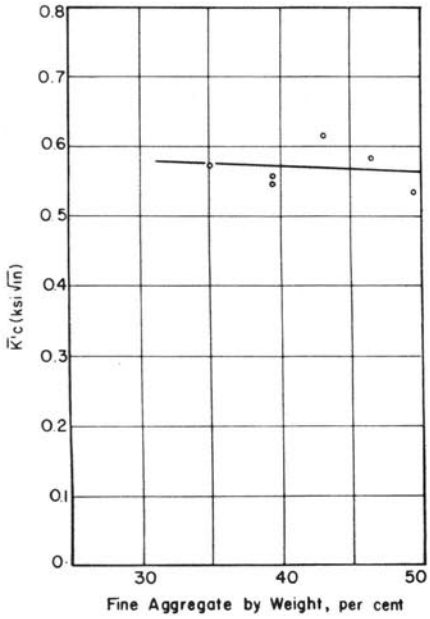

FIGURE 9. EFFECT OF FINE AGGREGATE ON $\bar{K}'_c$: CONCRETES

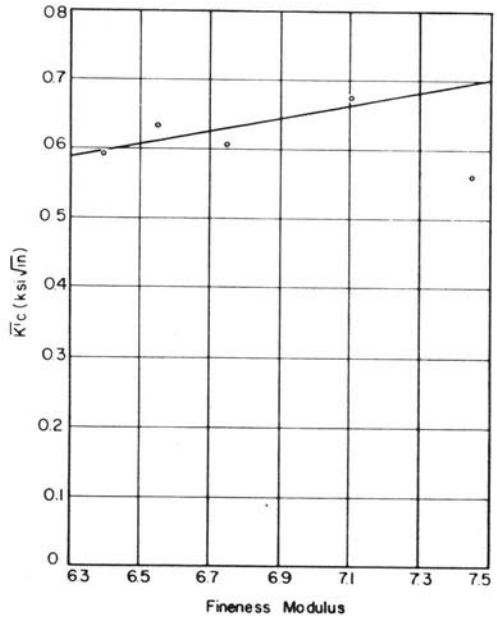

FIGURE 10. EFFECT OF FINENESS MODULUS OF COARSE AGGREGATE ON $\bar{K}'_c$: CONCRETES

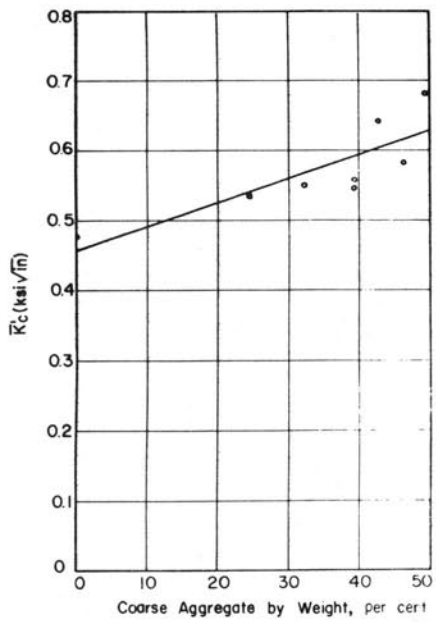

FIGURE 11. EFFECT OF COARSE AGGREGATE ON $\bar{K}'_c$: CONCRETES

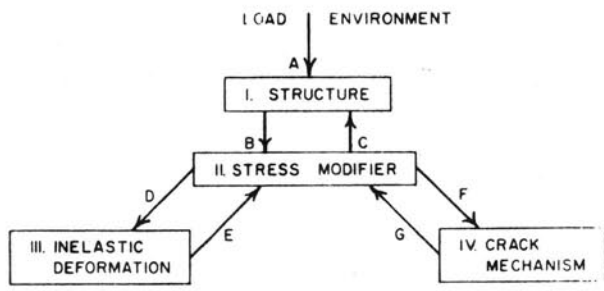

FIGURE 12. SCHEMATIC OF FRACTURE SYSTEM

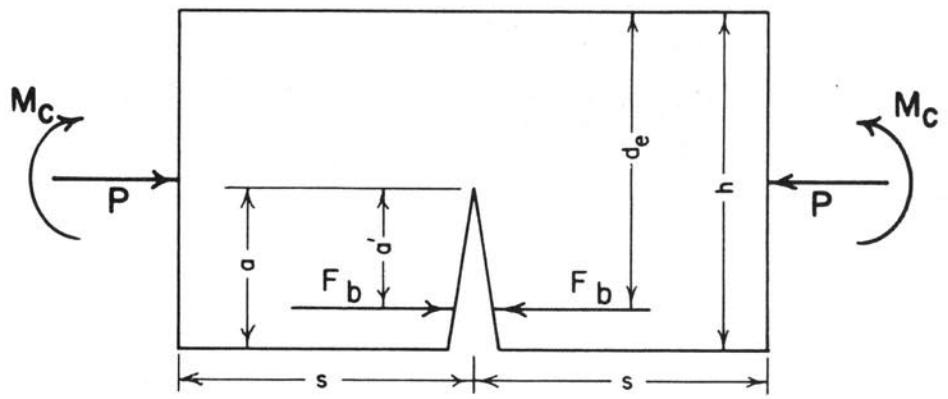

FIGURE 13. CRACKED CONCRETE ELEMENT FROM REINFORCED CONCRETE BODY

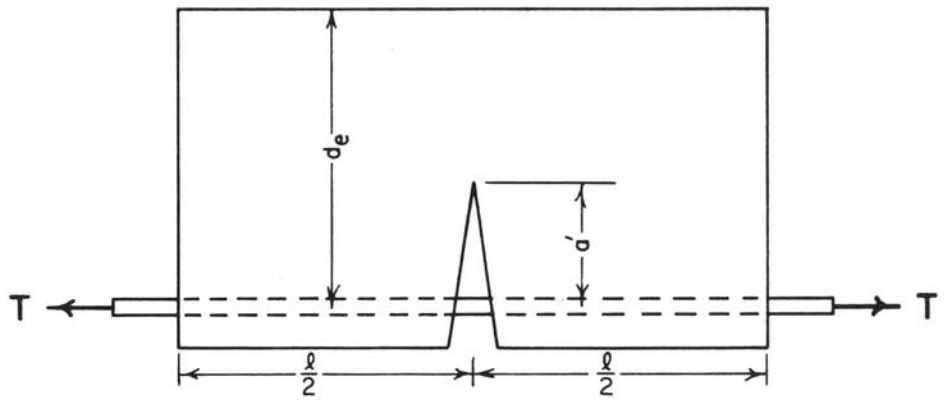

FIGURE 14. REINFORCED CONCRETE TENSION MEMBER

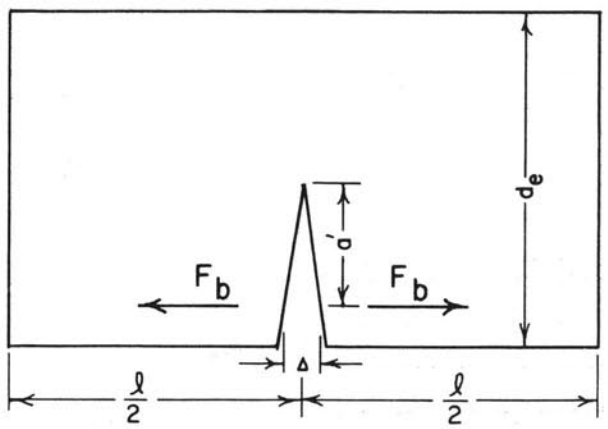

FIGURE 15. CRACKED CONCRETE ELEMENT FROM TENSION MEMBER

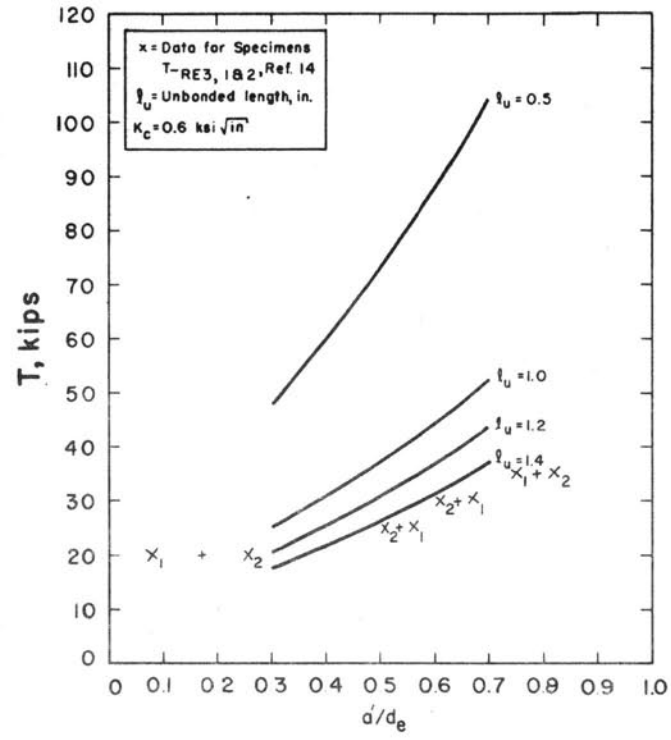

FIGURE 16. LOAD, T, VS a/d_e FOR DIFFERENT UNBONDED LENGTHS, ℓ_u

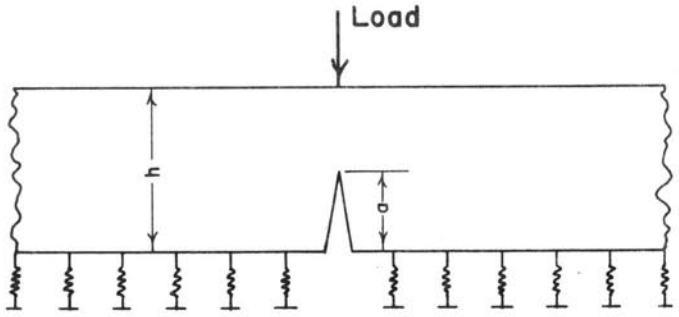

FIGURE 17. CRACKED RIGID PAVEMENT

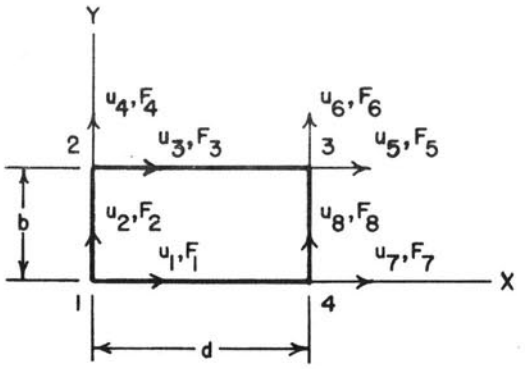

FIGURE 18. A TYPICAL ELEMENT

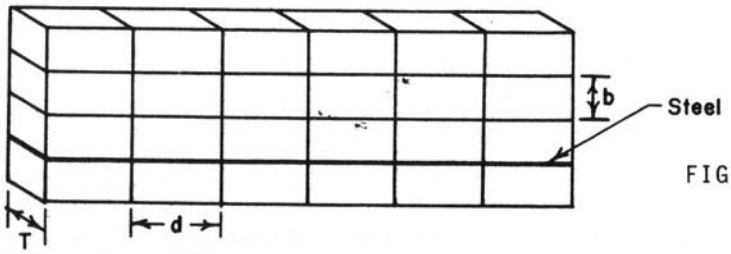

FIGURE 19. REINFORCED CONCRETE MODEL

$$[F] = \left(\int_v [B]^T [C][B] \, dV \right) [u] \qquad (17)$$

where [F] is a column matrix representing the forces at the four nodal points of the element, $[D]^T$ is the transpose of [D], and the remaining expressions are as defined above.

The final equation can be expressed in matrix notation as follows:

$$[F] = [K][u] \qquad (17a)$$

where:

$$[K] = \int_v [D]^T [C][D] \, dV.$$

[K] is called the stiffness matrix for one element and it relates the nodal point forces to the nodal point displacements. The stiffness matrix of the entire system can be obtained by directly adding the contribution of each individual element stiffness in the proper location.

4.2.6 Incorporation of Shrinkage Strains in the Model

The free shrinkage strain at any point in an element is a function of the relative humidity at that point. For purposes of consistency of the displacements u_x, u_y, the shrinkage strains for a specimen drying from one side only are assumed to be defined by the following formulas:

$$\begin{aligned} \varepsilon_{xs} &= a_1 + a_2\eta \, , \\ \varepsilon_{ys} &= a_1 + a_2\eta \, , \\ \gamma_{xys} &= 0 \, , \end{aligned} \qquad (18)$$

where:

ε_{xs} = normal shrinkage strain in x-direction

ε_{ys} = normal shrinkage strain in y-direction

γ_{xys} = shearing shrinkage strain,

a_1 and a_2 = constants,

η = y/b.

Equation (18) can be written in matrix notation as:

$$[\varepsilon_1] = \begin{bmatrix} \varepsilon_{xs} \\ \varepsilon_{ys} \\ \gamma_{xys} \end{bmatrix} \qquad \begin{bmatrix} a_1 + a_2\eta \\ a_1 + a_2\eta \\ 0 \end{bmatrix} \qquad (18a)$$

The reason for assuming ε_{xs} and ε_{ys} being equal at any particular point in the element is that these shrinkage strains are very similar in nature to thermal strains. Other assumptions concerning the distributions of shrinkage stresses can be incorporated into the analysis.

The forces that are induced at each node as a result of the shrinkage strains must be found in order to incorporate the effect of shrinkage strains in the model. Consider Figure 18 and assume that the element is acted upon by a state of shrinkage strain of the type described above. The forces produced by this state of strain can be found by using the fact that the work done by the external forces must equal the change of the internal energy.

$$[F_s]^T[u] = \int_v [\sigma_s]^T[\varepsilon] \, dV \qquad (19)$$

where:

[u] = matrix of unit displacements at the nodes of the element;

$[F_s]^T$ = transpose of the matrix of forces that are produced at the nodes as a result of shrinkage strains;

$[\sigma_s]^T$ = transpose of the matrix of stresses produced by shrinkage strains;

$[\varepsilon]$ = matrix of strains produced by unit displacements at the nodes; $[\varepsilon] = [D]$ since the magnitude of the displacement is unity;

dV = element of volume in the element;

$\int_V$ = integration over total volume of the element.

From the stress-strain relationship

$$[\sigma_s] = [C][\varepsilon_1]$$

and

$$[\sigma_s]^T = [\varepsilon_1]^T[C]^T ,$$

however, since $[C]$ is a symmetric matrix $[C]^T = [C]$. Therefore,

$$[\sigma_s]^T = [\varepsilon_1]^T[C] \qquad (20)$$

The forces resulting from shrinkage strains can be found by substituting Equation (20) into Equation (19), thus

$$[F_s]^T = \int_V [\varepsilon_1]^T[C][D]\, dV. \qquad (21)$$

The final equation that relates nodal forces to nodal displacements and shearing strains is

$$[F] = [K][u] + [F_s]. \qquad (22)$$

As a result of shrinkage strains, nodal forces are produced which may be obtained for the entire model by adding the contributions of individual elements in the proper locations. The equation relating nodal forces to nodal displacements and shrinkage strains for the entire model is

$$[\underline{F}] = [\underline{K}][\underline{u}] + [\underline{F_s}] \qquad (23)$$

where:

$[\underline{F}]$ = a 2n x 1 column matrix of forces at all nodes;

$[\underline{K}]$ = a 2n x 2n symmetrical stiffness matrix for the entire body;

$[\underline{u}]$ = a 2 n x 1 column matrix of displacements at all nodes;

$[\underline{F_s}]$ = a 2n x 1 column matrix of forces induced at nodal points by shrinkage strains;

n = total number of nodes.

Equation (23) represents a system of 2n simultaneous equations which can be solved for the nodal displacements. These equations are derived from the force equilibrium equations in the x- and y-directions, i.e., the sum of all the forces in the x- and y-directions at any node must equal zero unless a boundary condition is defined at the node. When a boundary condition is defined at a node the sum of the forces at the node will equal the external load applied at that node.

4.2.7 Development of Cracks

Stresses are calculated at five points for every element -- the four corners and the center of the element. The principal stresses and the direction of the maximum principal stress are calculated at the center of every element. The maximum principal stress at the center is compared to a limiting stress for cracking and if it exceeds the limiting stress, the element is assumed to have cracked and thus does not carry any tensile stresses. When cracking does occur, the element can be completely ignored since the loading is assumed to be one directional. If the stresses in two or more horizontally adjacent elements exceed the limiting stress at the same time, the element with the largest stress is assumed to be cracked. Cracks are found through an iteration process and every time a new crack appears the analysis is repeated in order to find other cracks

that might have appeared as a result of the new crack. Thus the crack pattern in the model is developed and the direction of each crack is also calculated. It should be noted, however, that since a cracked element is assumed to carry no stress, no two horizontally adjacent elements can be cracked. This requires that the length of each element not exceed one-half of the expected crack spacing.

4.3 APPLICATION OF THE METHOD AND BOUNDARY CONDITIONS

4.3.1 Application of Method

The method developed can be applied to any member with a shape that can be approximated by rectangular elements. The assumptions that were made in developing the method must also be reasonably valid, i.e., since it is assumed that the stress-strain diagram for concrete is linear, the maximum compressive stress in the concrete must remain below a reasonable limit.

The loads are applied to the nodes and the directions of the loads are governed by the set of axes assumed for the model, i.e., loads acting in the positive x- and y-directions are assumed positive. If there are any applied displacements, they follow the same sign convention. Volume change strain is applied to the elements and two values of volume change strain are specified, one at the top side and one at the bottom side of the element. It is assumed that there is a linear strain variation between the two values of volume change strain for the element. It is further assumed that all of the elements in a row are under the influence of the same shrinkage strain. The volume change strain is assumed to be positive if it produces expansion and negative if it produces contraction.

The steel stresses are limited by the assumption of perfect bond between the steel and concrete.

The method is not limited to concrete but can be used to evaluate the stresses for any material.

4.3.2 Boundary Conditions

Boundary conditions are limited only in the sense that the conditions are applied at the nodes. To represent a roller, the vertical displacement at the node on the roller is set equal to zero. To represent a pin connection, both the horizontal and vertical displacements at the node are set equal to zero. To represent a fixed end, the horizontal and vertical displacements of all the nodes at that end are set equal to zero. Other boundary conditions may be applied similarly. Boundary conditions that partially limit the movement of a node, such as a spring, can be applied if modifications are made in the digital computer program.

4.3.3 Computer Program for Deterimination of Volume Change Stresses in Plain and Reinforced Concrete Using Finite Element Analysis

The computer program VCSC (Volume Change Stresses in Concrete), prepared in FORTRAN IV, and a User's Manual are contained in the Appendix.

V. PRACTICAL APPLICATIONS

5.1 EFFECT OF CONCRETE PARAMETERS ON FRACTURE TOUGHNESS

The effective fracture toughness was not significantly affected by the fine aggregate content (30.0 per cent to 50.0 per cent, by weight), air content (4.0 per cent to 10.0 per cent), and water-cement ratio (5.7 gal/sack to 7.3 gal/sack). Since the range of the parameters investigated was inclusive of most mix designs, they can be neglected in designing for a mix of high or low fracture toughness (material's resistance to propagation of an existing flaw). Although only two types of coarse aggregate were used in the investigation, the results suggest that the effect of type of coarse aggregate on the fracture toughness was similar to the effect of type of coarse aggregate on the bond strength between coarse aggregate and cement paste or mortar.[16] Thus, high quality aggregates (homogeneous, low absorption, high modulus of elasticity relative to cement paste, etc.) should be used to develop mixes with high fracture toughness values (gradation requirements previously stated would apply to all types of aggregate). The variables significantly affecting the fracture toughness of concrete can be limited to the coarse aggregate content and gradation of coarse aggregate.

The effective fracture toughness of concrete was found to be directly proportional to both coarse aggregate content and gradation of coarse aggregate. Thus, by increasing or decreasing the percentage of coarse aggregate, or increasing or decreasing the maximum aggregate size, or a combination of both, the fracture toughness can be adjusted. However, if the fracture toughness is to be increased by using a larger maximum size coarse aggregate, the gradation of coarse aggregate must be uniform to minimize segregation and its detrimental effects. Limitations will be placed on maximum aggregate size by design considerations, i.e., size and shape of the concrete members, amount and distribution of reinforcing steel, etc.

Since the major aim of crack control is to minimize crack width by increasing the number of cracks in hardened concrete, the design of a concrete mix to maximize the high fracture toughness is not necessarily the answer. It also may be advisable to make a sacrifice in the desired fracture toughness value so that small flaws can form to act as stress relievers. These small flaws would prevent the buildup of stress values in the concrete that can lead to formation of large cracks which could allow the ingress of water

to cause corrosion of the reinforcement which could then result in rapid deterioration of the concrete. However, in the design of all mixes the objectives of required qualities of hardened concrete, workability of fresh concrete, and economy should be maintained even if it means a sacrifice in fracture toughness.

5.2 CRACK MECHANISM FOR CONCRETE STRUCTURES

In order to control the cracking of concrete structures due to varying load and environment, a systems-type analysis can be used to describe the complex cracking mechanism for a reinforced concrete beam subjected to a constant moment, for a reinforced concrete member with the steel loaded in tension, and for a cracked beam on an elastic foundation.

A reinforced beam subjected to a constant moment may be analyzed using the approach developed. The resultant stress intensity factor is the sum of the individual stress intensity factors for the concrete being subjected only to a moment, for the concrete being subjected only to axial forces, and for the concrete being only subjected to the resultant forces at the level of the reinforcement. Since expressions for the individual stress intensity factors are available in the literature[11,12] the resultant stress intensity factor can be determined. When the resultant stress intensity factor becomes equal to or exceeds the critical stress intensity factor the crack will propagate until it is arrested.

The cracking mechanism in beams can be approximated by using a reinforced concrete member with the steel loaded in tension. Since the only forces acting on the concrete are the bond forces which develop as the reinforcement elongates, the stress intensity factor can be expressed in terms of either the bond forces or the crack opening displacement at the level of the reinforcement. The total force transmitted across the cracked section for equilibrium conditions for a given crack length and different lengths of unbonding can be calculated from the specimen geometry and material properties for the cracked specimen.

Cracking in rigid pavements may be analyzed by using a cracked beam on an elastic foundation. The stress intensity factor varies inversely with crack length since an increase in the crack length transfers more load to the structure in the region of the crack and thus reduces the stresses on the cracked section. This crack growth arrests additional cracking until the load is increased. The limiting condition is reached when the crack has propagated through the pavement depth while the load is still transferred to the foundation (stable crack growth condition). Also, this model finds application to crack growth under repeated random loads in rigid concrete pavements, but quantitative results cannot be derived until data becomes available on the change in crack length as a function of stress intensity factor related to repeated loads.

5.3 ANALYTICAL STUDY OF CRACK DEVELOPMENT ASSOCIATED WITH VOLUME CHANGE

The computer program VCSC (Volume Change Stresses in Concrete) is prepared

in FORTRAN IV for the solution of stresses caused by volume change in plain and reinforced concrete. The program is capable of solving cases in which the model is subjected to external and/or internal displacements as well as volume change strains. The program uses the finite element method of analysis. The elements are rectangles of equal size. Nodal displacements, normal stresses, and shearing stress at each node of each element, normal stresses, shearing stress, maximum principal stress, minimum principal stress, and direction of maximum principal stress at the center of the same element, and steel stresses for each element of steel result from the solution of each problem in the order given.

In their early life, highway pavements and bridge decks are subjected to shrinkage stresses that may be the primary stresses acting on the members and may lead to cracks if the rate of drying is rapid enough. Under such conditions this method can be used to predict cracking patterns and stress distributions for various strengths of concretes, amount of reinforcement, and thickness of concrete cover, when the shrinkage stresses are dominant.

The boundary conditions used to simulate a bridge deck or a highway pavement could be rollers on the bottom of the model with a corner node fixed in both the x- and y- directions. The model should be long enough so the computation of stresses and displacements would converge to their actual values over a range of length which is sufficiently long for a crack pattern to develop. In general it is suggested that the stresses and deformations not be taken at points which are closer than two columns of elements to a side boundary.

VI. SUMMARY AND CONCLUSIONS

6.1 OBJECT AND SCOPE

The objective of this study is to gain an increased understanding of crack initiation and growth in concrete, which is essential to improved control of cracking of concrete structures, i.e., to acquire a better understanding of the effect of concrete parameters on crack development in concrete and to correlate crack development in concrete with various types of distress.

The investigation was divided into three major divisions: (1) experimental investigation of fracture toughness, effect of concrete parameters on the fracture toughness of pastes, mortars, and concretes; (2) crack mechanism for concrete structures, systems-type analysis description of complex cracking mechanism that occurs in concrete structures; and (3) analytical study of crack development associated with volume change, approximate solution for problem of shrinkage stresses in plain and reinforced concrete was developed.

6.2 RESULTS OF INVESTIGATION

6.2.1 Effect of Concrete Parameters on Fracture Toughness

The effective fracture toughness K_c' was based on the assumption that the concrete was homogeneous and the flaw depth at failure was equal to the cast flaw depth.

In the paste and mortar series there was a decrease in effective fracture toughness with increasing water-cement ratio, while in the concrete series there was no apparent effect of varying the water-cement ratio on effective fracture toughness for the range of water-cement ratios investigated.

Increasing the air content decreased the effective fracture toughness for the paste, mortar, and concrete series.

In the paste, mortar, and concrete series there was an increase in effective fracture toughness with age. This increase was significant up to an age of 29 days, but for curing times of greater than 29 days the change in effective fracture toughness from the 29-day value was not significant.

There was an increase in effective fracture toughness in the mortar series with increasing sand-cement ratio, however, the change in effective fracture toughness with increasing sand-cement ratio in the concrete series was not significant for the range of sand-cement ratios investigated.

The effective fracture toughness of the concrete series increased with an increase in the maximum size of coarse aggregate and also with an increased gravel-cement ratio. However, there was a decrease in the effective

fracture toughness when a large amount of maximum size aggregate was used in the mix. This was probably attributable to segregation.

The effective fracture toughness of the concrete series cast with a river gravel coarse aggregate was lower than the effective fracture toughness of the concrete series cast with a crushed limestone coarse aggregate for ages of three days and six days; however, at ages of 29 days and 92 days the difference in their effective fracture toughness was not significant.

6.2.2 Crack Mechanism for Concrete Structures

A fracture system of processes that respond to outside stimuli and interact was developed to describe the complex cracking mechanism in concrete structures. The system was applied to the free body diagram of the concrete portion of the structure, which is the structural element that contains the crack that will propagate.

The cracking mechanism in a reinforced concrete beam subjected to a constant moment was analyzed. A qualitative analysis of the cracking indicated that the resultant stress intensity factor which describes the stress field surrounding the crack in the beam was a function of the stress intensity factor due to the concrete being subjected only to a moment (causes crack extension), the stress intensity factor due to the effect of an axial load (negative for compressive forces and thus tends to arrest crack propagation), and the stress intensity factor due to the resultant forces at the level of the steel (negative when the bond forces act toward the crack thus causing crack arrest, and positive when load forces act away from the crack to cause crack propagation). Crack propagation occurs when the resultant stress intensity factor reaches the critical value.

A model was presented for investigating the cracking mechanism in beams. The model was used for a quantitative analysis of crack equilibrium. The only forces acting on the element are the bond forces, which can be examined by the opening displacement at the level of the reinforcement and are affected by unbonding. The stress intensity factor can be expressed in terms of the displacement, or the bond forces. Applying the results of this approach to the specimen geometry and material properties of Reference (14) yielded the following:

(a) The equilibrium crack length increases with the total force transmitted across the cracked section by the concrete and steel if the unbonded length is constant;

(b) The total force transmitted across the cracked section by the concrete and steel decreases as the unbonded length increases;

(c) An increased unbonded length is associated with an increased crack length during a virtual load increase.

The cracking in rigid pavements can be analyzed using a cracked beam on an elastic foundation. The stress intensity factor would vary inversely with the crack length since an increase in the crack length transfers more load to the elastic foundation in the region of the crack and reduces the stresses on the cracked section.

6.2.3 Analytical Study of Crack Development Associated with Volume Change

An analytical method for the evaluation of volume change stresses was presented which can be used for both plain and reinforced concrete. The finite element method was utilized with the aid of a digital computer program to construct an approximate solution to the problem. The method predicts cracking, crack patterns, and magnitude and distribution of stresses in members in which shrinkage stresses are the primary stresses.

The effects of various parameters on volume change stresses can be predicted. For example, the effect of concrete strength, concrete cover, amount of reinforcement, etc., can be studied by using various parameters in the computer program, thus saving considerable time over that required in an extensive experimental program.

The method can also consider the effects of loads and displacements on the model.

The method will be more effective as additional input data on shrinkage, particularly nonuniform shrinkage, become available. If reliable information on shrinkage strains at various times becomes available, then time to cracking can be predicted.

The bond between steel and concrete was assumed to be perfect. As a first approximation this is justifiable because volume change stresses are relatively small.

6.3 CONCLUSIONS

The results of this investigation can be used to describe the cracking of concrete structures due to various types of distress, i.e., distresses due to environment or loading. The resistance to propagation of the flaws inherent in concrete can be adjusted by modifying the mix design, i.e., varying the coarse aggregate content or gradation of coarse aggregate, or type of coarse aggregate. Since the experimental investigation covered a range of concrete parameters that would be inclusive of most mix designs, an approximate effective fracture toughness value can be determined from this investigation for most designs used.

From the effective fracture toughness value for the mix design chosen and the stress intensity factors due to the type of load distress, the resultant stress intensity factor can be determined for a reinforced concrete beam subjected to a constant moment. The resultant stress intensity factor can then be used to describe the cracking mechanism; i.e., crack propagation, which will occur when the resultant stress intensity factor reaches the critical value.

The model developed for investigating the cracking mechanism in concrete beams under load can be used for obtaining quantitative results. As an example of its application, this approach was used in conjunction with the results of Reference (14) for studying the equilibrium crack mechanism in reinforced concrete members.

Cracking in rigid pavements due to external load can be studied using a cracked beam on an elastic foundation. This model can also be used for studying the crack mechanism of pavements due to random loading, but further data is required on the change in stress

intensity factor with loading cycles.

The computer program developed can be used for evaluation of volume change stresses resulting from either environmental distress or load distress. The method predicts cracking, crack patterns, and magnitude and distribution of stresses in members in which shrinkage stresses are the primary stresses. The effects of various parameters on volume change stresses, as well as the effects of concrete cover, concrete strength, amount of reinforcement, etc., can be studied by using various parameters in the program.

VII. SUGGESTIONS FOR FUTURE RESEARCH

The effects of different environmental conditions and different loading rates on the effective fracture toughness of concrete should be investigated.

Application of the systems-type fracture analysis requires: understanding the inelastic phenomenon of unbonding of cracked sections; theoretical or empirical knowledge of the actual concrete stresses near cracks; development of stress intensity factor expressions for various models such as the rigid pavement; and a further look at fatigue crack growth in terms of the stress intensity factor with loading cycles.

Utilization of the analytic method for solution of volume change stresses requires data which is compatible with the computer program. One area in which there is insufficient data is shrinkage strains in members of large cross section so that nonuniform shrinkage data can be obtained with all but one or two surfaces sealed. Data should be provided for free shrinkage versus time for various drying, environmental, and surface conditions. A load-slip relationship could be incorporated into the program to eliminate the assumption of perfect bond between the steel and concrete, and thus bond stress can be part of the program output. The computer program could be modified to accept springs as part of the boundary conditions so that slip over the subgrade of the highway pavement can be incorporated. Also, in order to investigate the effects of rate of drying on the stresses produced by shrinkage, the shape of the stress-strain curve could be varied, i.e., study the effect of the stress-strain diagram on the effect of the maximum value of strain which occurs at the outermost fiber of the member.

VIII. REFERENCES

(1) "Fracture Toughness Testing and Its Applications," ASTM STP No. 381, American Society for Testing and Materials (April, 1965).

(2) Irwin, G. R. Proceedings, 1960 Sagamore Research Conference on Ordnance Materials. Washington, D.C.: U.S. Office of Technical Services.

(3) Kaplan, M. F., "Crack Propagation and the Fracture of Concrete," Proceedings, American Concrete Institute, 58 (1961), pp. 591-611.

(4) Glucklich, J., "Fracture of Plain Concrete," Proceedings of the ASCE, 89:EM 6 (1963), pp. 127-138.

(5) _____, "Static and Fatigue Fractures of Portland Cement Mortars in Flexure," Proceedings, First International Conference on Fracture, Vol. 2, Sendai, Japan (1965), pp. 1343-1382.

(6) Lott, J. L. and Kesler, C. E., "Crack Propagation in Plain Concrete," Symposium on Structure of Portland Cement Paste and Concrete, Highway Research Board Special Report 90, Washington, D.C., (1966), pp. 204-218.

(7) Naus, D. J. and Lott, J. L., "Fracture Toughness of Portland Cement Concretes," Theoretical and Applied Mechanics Report No. 314, University of Illinois at Urbana-Champaign (1968), pp. 1-87.

(8) Brown, W. F. and Srawley, J. E., "Plane Strain Crack Toughness Testing of High Strength Metallic Materials," ASTM STP No. 410, American Society for Testing and Materials (1966), pp. 13-14.

(9) Powers, T. C. and Brownyard, T. L., "Studies of the Physical Properties of Hardened Portland Cement Paste," Proceedings, American Concrete Institute, 41, (1946-7), pp. 101-132, 249-503, 549-602, 669-712, 845-880, 992-993.

(10) Hahn, G. T. and Rosenfield, A. R., "A Systems-Type Approach to Problems on Fracture" in Fundamental Phenomena in the Material Sciences, Vol. 4. New York: Plenum Press (1967), pp. 33-43.

(11) Srawley, J. E. and Gross, B., "Stress Intensity Factors for Crack-line-Loaded Edge-Crack Specimens," NASA TND - 3820 (1967), pp. 1-19.

(12) Gross, B., Roberts, E., Jr., and Srawley, J. E., "Elastic Displacements for Various Edge-Cracked Plate Specimens," NASA TND-4232 (1967), pp. 1-12.

(13) Reis, E. E., Jr., Mozer, J., Bianchini, A. C., and Kesler, C. E., "Causes and Control of Cracking in Concrete Reinforced with High Strength Steel Bars--A Review of Research," University of Illinois Engineering Experiment Station Bulletin No. 479, Urbana, Illinois (1965), pp. 1-61.

(14) Broms, B. B., "Stress Distribution, Crack Patterns and Failure Mechanisms of Reinforced Concrete Members," Proceedings, American Concrete Institute, 61 (October, 1964), pp. 1535-1557.

(15) Pzemieniecki, J. S. Theory of Matrix Structural Analysis. New York: McGraw-Hill Book Co., (1968).

(16) Hsu, T. T. C. and Slate, F. O., "Tensile Bond Strength Between Aggregate and Cement Paste or Mortar," Proceedings, ACI, Vol. 60 (April, 1963), pp. 465-486.

IX. APPENDIX I: USER'S GUIDE FOR COMPUTER PROGRAM IN FORTRAN IV

User's Guide

The computer program VCSC (Volume Change Stresses in Concrete) is prepared in FORTRAN IV language for the solution of "Stresses Caused by Volume Change in Plain and Reinforced Concrete." The program is capable of solving cases in which the model is subjected to external loads and/or external displacements as well as volume change strains. The program uses the finite element method of analysis. The elements are rectangles of equal size. The result of the solution of each problem is the nodal displacements, the normal stresses, and the shearing stress at each node of each element; the normal stresses, the shearing stress, the maximum principal stress, the minimum principal stress, and the direction of maximum principal stress at the center of the same element; and steel stresses for each element of steel, in that order.

The input for the program consists of the following parameters:

(a) The controlling information for the geometry and input and output of the results;

(b) description of material properties;

(c) numerical values for external loads, external displacements, and volume change strains.

The input cards for the program are discussed below in the order that they appear in the program:

```
      READ 242, NPBLM;
  242 FØRMAT (I5).
```

The value of NPBLM indicates the number of problems that are to be solved. This will be discussed in more detail later.

```
 1000 READ 1, MX, NX, DX, DY, ANU,
      E, ES, AS, LFSN, LSN, KIND,
      NSTR
    1 FØRMAT (2I5, 3F5.2, 2F15.1,
      F5.3, 4I5)
```

where:

MX = number of elements in each row.

NX = number of elements in each column.

DX = the length of an element.

DY = the height of an element.

ANU = Poisson's ratio for concrete.

E = modulus of elasticity of concrete.

ES = modulus of elasticity of steel.

AS = the area of steel.

LFSN = the first steel node.

LSN = the last steel node.

KIND = 0 is the problem is plane strain, = any non-zero number up to five digits if the problem is plane stress.

NSTR = number of points in an element

at which the stresses are to be evaluated. This is either 1 or 5 for evaluating the stresses at the center of the element or at the center and the four corners, respectively.

The value of NPBLM is equal to the number of cards that correspond to the 1000 READ 1 statement.

```
      READ 166, NANLYS, SIGCR, AINC
  166 FØRMAT (15, 2F10.5)
```

where:

NANLYS = the number of times a problem is to be repeated with the load or displacement incremented each time, or with shrinkage strains increased.

SIGCR = limiting tensile stress for concrete.

AINC = the increment by which the loads or displacements are to be increased, represented as a fraction of the original loads or displacements.

```
      READ 310, N
  310 FØRMAT (15)
```

The number N represents the total number of nodes at which a particular displacement is to be defined such as supports. For example, for a simply supported beam, the value of N would be 2 for the two nodes that are restrained in one or both directions, unless displacements are also applied at other nodes.

```
      READ 303, JK, KZ1, PLOAD (2*JK-1),
      KZ2, PLOAD(2*JK)
  303 FØRMAT (215, F10.5, 15, F10.5)
```

where:

JK = the number of node at which there is to be a displacement constraint.

KZ1 = 1 if there exists a constraint in the x-direction at node JK; 0 if there is no constraint in the x-direction at node JK.

PLOAD (2*JK-1) = the magnitude of the displacement constraint in the x-direction, zero for supports

KZ2 = 1 if there is a constraint in the y-direction at node JK; 0 if there is no constraint in the y-direction at node JK.

PLOAD (2*JK) = the magnitude of the displacement constraint in the y-direction, zero for supports.

```
      READ 310, N
  310 FØRMAT (15)
```

Here, the number N represents the total number of nodes at which loads are applied.

```
      READ 312, JK, KZ1, PPLOD(2*JK-1),
      KZ2, PPLOD(2*JK)
  312 FØRMAT (215, F10.5, 15, F10.5)
```

where:

JK = the number of the node at which a load is to be applied.

KZ1 = 1 if there is a load component in the x-direction at node JK; 0 if there is no load component in the x-direction at node JK.

PPLOD (2*JK-1) = magnitude of the load in the x-direction at node JK.

KZ2 = 1 if there is a load component in the y-direction at node JK; 0 if there is no load in the y-direction at node JK.

PPLOD (2*JK) = magnitude of the load in the y-direction at node JK.

```
      READ 400, M
  400 FØRMAT (15)
```

The number M is the total of all the rows of nodes at which volume change strains are to be applied.

```
      READ 403, (SHRKG(I), I = 1, M)
  403 FØRMAT (5F15.10)
```

where:

SHRKG(I) = the value of volume change strain at the rows of nodes I.

I = the number of the row for which the strain is being read; the top row of nodes is number 1, the second row number 2, and so on.

This concludes the definition of the READ statements.

The following is an explanation of

the PRINT statements in the computer program except for those print statements that comprise the titles for the printed output:

```
      PRINT 69, MX, NX, DX, DY, ANU,
     E, ES, AS, LFSN, LSN, KIND,
     NSTR
   69 FØRMAT (215, 3F5.2, 2F15.1,
     F5.3, 415//)
      PRINT 660, NANLYS, SIGCR, AINC
  660 FØRMAT (I19, F17.5, F16.5//)
      PRINT 661, JK, KZ1, PLOAD
     (2*JK-1), KZ2, PLOAD(2*JK)
  661 FØRMAT (I6, I13, F17.5, I13,
     F16.5//)
      PRINT 662, JK, KZ1, PPLOD
     (2*JK-1), KZ2, PPLOD(2*JK)
  662 FØRMAT (I6, I6, F13.2, I6,
     F12.2//)
      PRINT 663, (SHRKG (I), I = 1,
     M)
  663 FØRMAT (5F15.10//)
```

The parameters are already defined in the explanation of the READ statements. These PRINT statements merely print out the input parameters for checking purposes.

```
      PRINT 314, K, EPOAD
  314 FØRMAT (I6, E15.6//)
```

where:

K = number of node at which an external load is applied.

EPOAD = the load acting at node K. This includes the increments to the loads if there are any.

```
      PRINT 314, K, ELOAD(2*K-2+IJ)
  314 FØRMAT (I6, E15.6)
```

where:

K = the number of node at which there exists a displacement constraint.

ELOAD (2*K-2+IJ) = the magnitude of the displacement constraint at node K. Zero for supports.

If a node number appears twice in this PRINT statement, the first constraint is in the x-direction and the second constraint is in the y-direction. This, for example, would happen for a node fixed in both directions for which the magnitudes would be zero in both directions. The magnitude of the displacement will include the additional increments, if any.

```
      PRINT 83, I, LCNT(I), NCR(I),
     ELD(I21), ELD(I22)
   83 FØRMAT (I6, I14, I26, E24.4,
     E13.4)
```

where:

I = the number of node

LCNT(I) = the total number of elements connected to node I

NCR(I) = the total number of cracked elements connected to node I. Note that NCR(I) must always be less than LCNT(I)

ELD(I21), ELD(I22) = the magnitude of displacements at node I in the x- and y-directions, respectively.

```
      PRINT 707, J, ((SIGMA (K1,I),
     K1 = 1, 3), I=2, NSTR)
  707 FØRMAT (I5, 6X, 12E10.3)
```

where:

J = the number of elements.

SIGMA = the stresses in the elements. Here a set of stresses is printed out for each node, 1, 2, 3, and 4, of the element. Each set of stresses consists of the stresses in the x- and y-directions and the shear stress.

```
      PRINT 18, J, ICR(J), (SIG(I, J),
     I = 1, 3), SIGP1, SIGP2, THETA
   18 FØRMAT (2I5, 2X, 3E13.4, 2X,
     2E13.4, F10.4/)
```

This is a PRINT statement for the stresses at the center of the element in which:

J = element number

ICR(J) = 0 if the element is not cracked,

>0 if the element is cracked

SIG = a set of stresses at the center of the element. The set consists of stresses in the x- and y-directions and the shear stress

SIGP1 = maximum principal stress at the center of the element

SIGP2 = minimum principal stress at the center of the element

THETA = the angle that the maximum principal stress makes with the positive direction of the x-axis, in degrees.

```
      PRINT 19, KCR, NCRT
   19 FØRMAT (I14, I25)
```

where:

KCR = the number of elements cracked in the immediately preceding round.

NCRT = the total number of elements cracked up to this point.

```
      PRINT 602, I, SIGST(I)
  602 FØRMAT (I15, E13.4)
```

where:

I = the number of steel element

SIGST(I) = the steel stress for the steel element I.

X. APPENDIX II: COMPUTER PROGRAM IN FORTRAN IV FOR DETERMINATION OF VOLUME CHANGE STRESSES IN PLAIN AND REINFORCED CONCRETE USING FINITE ELEMENT ANALYSIS

```
/*ID            HASSAN M. REJALI
//              EXEC WATFOR
//SYSIN         DD *
$JOB            KP=26,TIME=300,PAGES=100
      DIMENSION  X(200),Y(200),NNE(400,4),LCNT(200),NEN(200,4),AK(8,8)
     1,STIF(2,200 ),KZ(700),KKH(1400),COEF(400,25),ELD(400),ELOAD(400),
     2SIG(3,400),DISP(8),CB(5,3,8),SHRKG(400),EPS(400,2),SIGMA(3,5),
     3SIGST(100),PLOAD(400),ICR(400),PPLOD(400),KA(700),NCR(400)
      T=1.0
      PI=3.14159265358979
      READ 242,NPRLM
 242  FORMAT(I5)
 1000 READ 1,MX,NX,DX,DY,ANU,E,ES,AS,LFSN,LSN,KIND,NSTR
 1    FORMAT (2I5,3F5.2,2F15.1,F5.3,4I5)
      PRINT 240
 240  FORMAT(1H1)
      PRINT 232
 232  FORMAT(/  INPUT DATA/)
      PRINT69,MX,NX,DX,DY,ANU,E,ES,AS,LFSN,LSN,KIND,NSTR
 69   FORMAT (2I5,3F5.2,2F15.1,F5.3,4I5//)
      READ  166,NANLYS,SIGCR,AINC
 166  FORMAT(I5,2F10.5)
      PRINT 692
 692  FORMAT(/  NUMBER OF PROBLEMS,  CRITICAL STRESS,  LOAD INCREMENT/)
      PRINT 660,NANLYS,SIGCR,AINC
 660  FORMAT(I19,F17.5,F16.5//)
C  FOR THE PURPOSE OF EVALUATION OF STIFFNESSES REPLACE E BY 1.
      MT=MX+1
      NT=NX+1
      EE=1.0
      STFR=(12.*ES*AS*EE)/(DX*E)
C  STFR IS THE STEEL FACTOR COMPARABLE TO AK/S FOR THE CONCRETE
C  COEFFICIENTS RELATING DISPLACEMENTS TO FORCES FOR A SINGLE ELEMENT
      ANU1=(1.-ANU)/((1.+ANU)*(1.-2.*ANU))
      ANU2=ANU/((1.+ANU)*(1.-2.*ANU))
      IF(KIND.EQ.0)  GO TO 701
      ANU1=1./(1.-ANU*ANU)
      ANU2=ANU/(1.-ANU*ANU)
 701  ANU3=1./2.*(1.+ANU)
      BETA=DY/DX
      AK(1,1)=4.*ANU1*BETA+4.*ANU3/BETA
      AK(1,2)=3.*(ANU2+ANU3)
      AK(2,1)=3.*(ANU2+ANU3)
      AK(1,3)=2.*ANU1*BETA-4.*ANU3/BETA
      AK(3,1)=2.*ANU1*BETA-4.*ANU3/BETA
      AK(1,4)=3.*(ANU3-ANU2)
      AK(4,1)=3.*(ANU3-ANU2)
      AK(1,5)=-2.*(ANU1*BETA+ANU3/BETA)
      AK(5,1)=-2.*(ANU1*BETA+ANU3/BETA)
      AK(1,6)=-3.*(ANU2+ANU3)
```

```
      AK(6,1)=-3.*(ANU2+ANU3)
      AK(1,7)=-4.*ANU1*BETA+2.*ANU3/BETA
      AK(7,1)=-4.*ANU1*BETA+2.*ANU3/BETA
      AK(1,8)=-3.*(ANU3-ANU2)
      AK(8,1)=-3.*(ANU3-ANU2)
      AK(2,2)=4.*ANU1/BETA+4.*ANU3*BETA
      AK(2,3)=-3.*(ANU3-ANU2)
      AK(3,2)=-3.*(ANU3-ANU2)
      AK(2,4)=-4.*ANU1/BETA+2.*ANU3*BETA
      AK(4,2)=-4.*ANU1/BETA+2.*ANU3*BETA
      AK(2,5)=-3.*(ANU2+ANU3)
      AK(5,2)=-3.*(ANU2+ANU3)
      AK(2,6)=-2.*(ANU1/BETA+ANU3*BETA)
      AK(6,2)=-2.*(ANU1/BETA+ANU3*BETA)
      AK(2,7)=3.*(ANU3-ANU2)
      AK(7,2)=3.*(ANU3-ANU2)
      AK(2,8)=2.*ANU1/BETA-4.*ANU3*BETA
      AK(8,2)=2.*ANU1/BETA-4.*ANU3*BETA
      AK(3,3)=4.*ANU1*BETA+4.*ANU3/BETA
      AK(3,4)=-3.*(ANU2+ANU3)
      AK(4,3)=-3.*(ANU2+ANU3)
      AK(3,5)=-4.*ANU1*BETA+2.*ANU3/BETA
      AK(5,3)=-4.*ANU1*BETA+2.*ANU3/BETA
      AK(3,6)=3.*(ANU3-ANU2)
      AK(6,3)=3.*(ANU3-ANU2)
      AK(3,7)=-2.*ANU1*BETA-2.*ANU3/BETA
      AK(7,3)=-2.*ANU1*BETA-2.*ANU3/BETA
      AK(3,8)=3.*(ANU2+ANU3)
      AK(8,3)=3.*(ANU2+ANU3)
      AK(4,4)=4.*ANU1/BETA+4.*ANU3*BETA
      AK(4,5)=-3.*(ANU3-ANU2)
      AK(5,4)=-3.*(ANU3-ANU2)
      AK(4,6)=2.*ANU1/BETA-4.*ANU3*BETA
      AK(6,4)=2.*ANU1/BETA-4.*ANU3*BETA
      AK(4,7)=3.*(ANU2+ANU3)
      AK(7,4)=3.*(ANU2+ANU3)
      AK(4,8)=-2.*ANU1/BETA-2.*ANU3*BETA
      AK(8,4)=-2.*ANU1/BETA-2.*ANU3*BETA
      AK(5,5)=4.*ANU1*BETA+4.*ANU3/BETA
      AK(5,6)=3.*(ANU2+ANU3)
      AK(6,5)=3.*(ANU2+ANU3)
      AK(5,7)=2.*ANU1*BETA-4.*ANU3/BETA
      AK(7,5)=2.*ANU1*BETA-4.*ANU3/BETA
      AK(5,8)=3.*(ANU3-ANU2)
      AK(8,5)=3.*(ANU3-ANU2)
      AK(6,6)=4.*ANU1/BETA+4.*ANU3*BETA
      AK(6,7)=-3.*(ANU3-ANU2)
      AK(7,6)=-3.*(ANU3-ANU2)
      AK(6,8)=-4.*ANU1/BETA+2.*ANU3*BETA
      AK(8,6)=-4.*ANU1/BETA+2.*ANU3*BETA
      AK(7,7)=4.*ANU1*BETA+4.*ANU3/BETA
      AK(7,8)=-3.*(ANU2+ANU3)
      AK(8,7)=-3.*(ANU2+ANU3)
      AK(8,8)=4.*ANU1/BETA+4.*ANU3*BETA
C  DETERMINATION OF THE COORDINATES OF THE NODAL POINTS
      MT1=MT-1
      NT1=NT-1
      DO  20  M=1,MT
      M1=M-1
      AM = M1
      DO 20 N=1,NT
      N1=N-1
      AN =N1
      L=M1*NT+N
```

```
      X(L) = AM*DX
      Y(L) = AN*DY
C  DETERMINATION OF THE NO. OF NODES FOR EACH ELEMENT AND NODE NUMBERS
 115  IF(M-1)  20,20,10
  10  IF(N-1) 20,20,151
 151  K1=(M-2)*NT1+(N-1)
      NNF(K1,1)=L-NT-1
      NNF(K1,2)=L-NT
      NNF(K1,3)=L
      NNF(K1,4)=L-1
  20  CONTINUE
      LT=L
      KT=K1
      DO21L=1,LT
      NCR(L)=0
  21  LCNT(L)=0
      DO 25 K=1,KT
      DO 25 I=1,4
      NI=NNF(K,I)
      LCNT(NI)=LCNT(NI)+1
      LC1=LCNT(NI)
  25  NEN(NI,LC1)=K
      DO 8  L=1,LT
      KA(L)=1
 8    KZ(L)=1
      READ 310,N
 310  FORMAT(I5)
      PRINT 233
 233  FORMAT(≠  NODE,  CONSTRAINT,  X-DISPLACEMENT,  CONSTRAINT,  Y-DISP
     1LACEMENT≠)
      DO 302 K=1,N
      READ 303,JK,KZ1,PLOAD(2*JK-1),KZ2,PLOAD(2*JK)
 303  FORMAT(2I5,F10.5,I5,F10.5)
      PRINT661,JK,KZ1,PLOAD(2*JK-1),KZ2,PLOAD(2*JK)
 661  FORMAT(I6,I13,F17.5,I13,F16.5//)
 302  KZ(JK)=1+KZ1+2*KZ2
      READ 310,N
      IF(N.EQ.0)  GO TO 455
      PRINT 234
 234  FORMAT(≠  NODE,  X-LOAD,  AMOUNT,  Y-LOAD,  AMOUNT≠)
      DO 315 K=1,N
      READ 312,JK,KZ1,PPLOD(2*JK-1),KZ2,PPLOD(2*JK)
 312  FORMAT(2I5,F10.5,I5,F10.5)
      PRINT662,JK,KZ1,PPLOD(2*JK-1),KZ2,PPLOD(2*JK)
 662  FORMAT(I6,I6,F12.2,I6,F12.2//)
 315  KA(JK)=1+KZ1+2*KZ2
 455  NSELT=(LSN-LFSN)/NT
      DO 401 L=1,KT
      ICR(L)=0
      EPS(L,1)=0.0
 401  EPS(L,2)=0.0
      NCRT=0
      DO 4 NS=1,NANLYS
      ANS=NS
      READ 400,M
 400  FORMAT (I5)
      IF (M.EQ.0)  GO TO 22
      READ403,(SHRKG(I),I=1,M)
 403  FORMAT (5F15.10)
      PRINT 235
 235  FORMAT(≠  SHRINKAGE STRAIN FROM TOP TO BOTTOM ON ROWS OF NODES≠)
      PRINT 663,(SHRKG(I),I=1,M)
 663  FORMAT (5F15.10//)
      DO 407  I=1,M
```

```
      LL=NT-I+1
      IF(I.EQ.1)  GO TO 405
      DO 404  JJ=1,MT1
      J=LL+(JJ-1)*NT1
404   EPS(J,2)=SHRKG(I)
405   IF(I.EQ.NT)  GO TO 407
      LL=LL-1
      DO 406 JJ=1,MT1
      J=LL+(JJ-1)*NT1
406   EPS(J,1)=SHRKG(I)
407   CONTINUE
22    KCR=0
      NSN=LFSN
      DO 300 K=1,LT
      ELOAD(2*K-1)=0.
      ELOAD(2*K)=0.
      IF (KA(K).EQ.1)  GO TO 300
      II=KA(K)/2
      PRINT 236
236   FORMAT(≠  NODE          FORCE≠)
      DO313 I=1,II
      IJ=KA(K)-II-(II-1)*(2-I)
      ELOAD(2*K-2+IJ)=PPLOD(2*K-2+IJ)*(1.+(ANS-1.)*AINC)*12./E
      EPOAD=ELOAD(2*K-2+IJ)*E/12.
313   PRINT 314,K,EPOAD
314   FORMAT(I6,E15.6//)
300   CONTINUE
      DO 11 K=1,LT
      KH=K
      KL=K
      LC1=LCNT(K)
      DO 2  I=1,LC1
      NE=NEN(K,I)
      DO  2 L=1,4
      IF(KL-NNE(NE,L))  6,6,7
 7    KL=NNE(NE,L)
 6    IF(KH-NNE(NE,L))  9,2,2
 9    KH=NNE(NE,L)
 2    CONTINUE
      KH=2*KH
      IF(K.EQ.1) GOTO5
      KK2=2*K-2
      IF(KH.LT.(2*K-2+KKH(KK2))) KH=2*K-2+KKH(KK2)
5     KL=2*KL-1
      K21=2*K-1
      K22=2*K
      KKH(K21  )=KH-2*K+1
      KKH(K22)=KH-2*K
      KHL=KH-KL+1
C   THE FOLLOWING IS THE PROCEDURE BY WHICH THE STIF. MATRIX IS EVALUATED
C   TWO EQUATIONS AT ATIME
      DO99  I=1,2
      DO99 J=1,KHL
99    STIF(I,J)=0.
      IF(NCR(K).GE.LC1)  GO TO 555
      NCR(K)=0
      DO 29 I=1,LC1
      NE=NEN(K,I)
      IF(ICR(NE).GT.0)  GO TO 28
      DO  3 L=1,4
      IF(K-NNE(NE,L))  3,23,3
 3    CONTINUE
 23   JJ=L
      DO  92  L=1,4
```

```
      NN=NNE(NE,L)
      KM=2*NN-KL
      DO  92 N=1,2
      DO  92 M=1,2
      KMM=KM+M-1
      JJ2=2*JJ+N-2
      LM2=2*L+M-2
   92 STIF(N,KMM)=STIF(N,KMM)+AK(JJ2,LM2)
      C11=T*DY*(ANU1+ANU2)/6.
      C22=T*DX*(ANU1+ANU2)/4.
      AJ1=1-2*(JJ/3)
      AJ2=(JJ/2)-2*(JJ/4)+1
      AJ3=1-2*((JJ/2)-2*(JJ/4))
      ELOAD(2*K-1)=ELOAD(2*K-1)-C11*AJ1*(EPS(NE,2)*(3.-AJ2)+EPS(NE,1)*
     1AJ2)*12.
      ELOAD(2*K)=ELOAD(2*K)-C22*AJ3*(EPS(NE,1)+EPS(NE,2))*12.
      GO TO 29
   28 NCR(K)=NCR(K)+1
   29 CONTINUE
  555 IF (K.NE.NSN.OR.NSN.GT.LSN)  GO TO 598
      IF(NCR(K).GE.LC1)  NCR(K)=NCR(K)+1
      NSN=NSN+NT
      STIF(1,2*K-KL)=STIF(1,2*K-KL)+2*STFR
      KST1=2*K-KL-2*NT
      KST2=2*K-KL+2*NT
      IF (K.EQ.LFSN) KST1=2*K-KL
      IF (K.EQ.LSN) KST2=2*K-KL
      STIF(1,KST1)=STIF(1,KST1)-STFR
      STIF(1,KST2)=STIF(1,KST2)-STFR
C    BONDARY CONDITIONS
      IF(NCR(K).EQ.LC1)  GO TO 11
  598 IF(KZ(K).EQ.1)  GO TO 76
      II=KZ(K)/2
      DO 87 I=1,II
      IJ=KZ(K)-II-(II-1)*(2-I)
      IF(NCR(K).GT.LC1.AND.IJ.EQ.2)  GO TO  556
      DO 88 JK=1,KHL
   88 STIF(IJ,JK) = 0.
      ELOAD(2*K-2+IJ)=PLOAD(2*K-2+IJ)*(1.+(ANS-1.)*AINC)
      PRINT 241
  241 FORMAT(#  NODE,  DISPLACEMENT#)
      PRINT 314,K,ELOAD(2*K-2+IJ)
   87 STIF(IJ,2*K-KL+IJ-1)=1.0
C  ELIMINATION OF THE OFF DIAGONAL TERMS
  556 IF(NCR(K).EQ.LC1)  GO TO11
   76 DO  100  I=1,2
      IF(NCR(K).GT.LC1.AND.I.EQ.2)  GO TO 11
      KI2=2*K-2+I
      KI21=KI2-1
      IF(K.EQ.1.AND.I.EQ.1)  GO TO 64
      DO  61  KK=KL,KI21
      KHK=KKH(KK)
      DO  62  JK=1,KHK
      KKL1=KK-KL+1
      JKKL=KKL1+JK
   62 STIF(I,JKKL) = STIF(I,JKKL)+STIF(I,KKL1)*COEF(KK,JK)
   61 ELOAD(KI2) = ELOAD(KI2)+STIF(I,KKL1)*ELD(KK)
   64 K2L1=KI2-KL+1
      ELD( KI2) = -ELOAD( KI2)/STIF(I,K2L1     )
      KKK2=KKH(KI2)
      IF(K.EQ.LT.AND.I.EQ.2)  GOTO 100
      DO 63 JJ=1,KKK2
      J2KL=JJ+KI2-KL+1
   63 COEF(KI2,JJ) = -STIF(I,J2KL)/STIF(I,K2L1)
```

```
 100   CONTINUE
 11    CONTINUE
C  BACK SUBSTITUTION AND EVALUATION OF THE DISPLACEMENTS CALLED -ELD-
       LT2 = 2*LT
       DO 81 K2=2,LT2
       NK=2*LT-K2+1
       KKK2=KKH(NK)
       DO 81 JJ=1,KKK2
       NKJ=NK+JJ
 81    ELD(NK) = ELD(NK)+COEF(NK,JJ)*ELD(NKJ)
       PRINT 999
 999   FORMAT (1H1)
       PRINT 34
 34    FORMAT(≠  NODE,  NO. OF ELEMENTS CONNECTED,  NO. OF ELEMENTS CRACK
      1ED,   DISPLACEMENTS  U,V≠)
       DO 900 I=1,LT2
 900   ELD(I)=-ELD(I)
       DO 85 I=1,LT
       I21 = 2*I-1
       I22=2*I
       PRINT 83,I,LCNT(I),NCR(I),ELD(I21),ELD(I22)
 83    FORMAT(I6,I14,I26,E24.4,E13.4)
 85    CONTINUE
C  EVALUATION OF THE STRESSES FROM THE DISPLACEMENTS
       PRINT 504
 504   FORMAT (1H1)
       DO 94  I=1,NSTR
       PSI=I/4
       ATA=I/3-I/5
       IF(I.GT.1)  GO TO 95
       PSI=0.5
       ATA=0.5
 95    PSI1=1.-PSI
       ATA1=1.-ATA
       PSI=PSI*E
       ATA=ATA*E
       PSI1=PSI1*E
       ATA1=ATA1*E
C  COEFFICIENTS RELATING DISPLACEMENTS TO STRESSES FOR A SINGLE ELEMENT
       CB(I,1,1)=-ANU1*ATA1/DX
       CB(I,1,2)=-ANU2*PSI1/DY
       CB(I,1,3)=-ANU1*ATA/DX
       CB(I,1,4)=ANU2*PSI1/DY
       CB(I,1,5)=ANU1*ATA/DX
       CB(I,1,6)=ANU2*PSI/DY
       CB(I,1,7)=ANU1*ATA1/DX
       CB(I,1,8)=-ANU2*PSI/DY
       CB(I,2,1)=-ANU2*ATA1/DX
       CB(I,2,2)=-ANU1*PSI1/DY
       CB(I,2,3)=-ANU2*ATA/DX
       CB(I,2,4)=ANU1*PSI1/DY
       CB(I,2,5)=ANU2*ATA/DX
       CB(I,2,6)=ANU1*PSI/DY
       CB(I,2,7)=ANU2*ATA1/DX
       CB(I,2,8)=-ANU1*PSI/DY
       CB(I,3,1)=-ANU3*PSI1/DY
       CB(I,3,2)=-ANU3*ATA1/DX
       CB(I,3,3)=ANU3*PSI1/DY
       CB(I,3,4)=-ANU3*ATA/DX
       CB(I,3,5)=ANU3*PSI/DY
       CB(I,3,6)=ANU3*ATA/DX
       CB(I,3,7)=-ANU3*PSI/DY
       CB(I,3,8)=ANU3*ATA1/DX
 94    CONTINUE
```

```
      PRINT 237
237   FORMAT(≠  ELEMENT NO.,  X,Y, AND SHEAR STERESSES AT FOUR CORNERS≠)
      PRINT 238
238   FORMAT(≠  ELEMENT NO.,  CRACKING NO.,  X,Y,  SHEAR STRESSES, MAX.,
     1 MIN. PRIN. STRESS, DIRECTION MAX. PRIN. STRESS AT CENTER≠)
      DO 101 J=1,KT
      DO 98 JH = 1,3
      SIG(JH,J)=0.0
      DO 98 I=1,5
98    SIGMA(JH,I)=0.0
      DO 97 I=1,4
      DISP(2*I-1)=FLD(2*NNE(J,I)-1)
97    DISP(2*I)=FLD(2*NNE(J,I))
      DO 103 I=1,NSTR
      DO 103 K1=1,3
      DO 102  K2=1,8
102   SIGMA(K1,I)=SIGMA(K1,I)+CB(I,K1,K2)*DISP(K2)
      II=-(I/3)+(I/5)+2
      IF(K1.EQ.3)  GO TO 104
      IF(I.EQ.1)  GO TO 972
      SIGMA(K1,I)=SIGMA(K1,I)-EPS(J,II)*(ANU1+ANU2)*E
      GO TO 103
972   SIGMA(K1,I)=SIGMA(K1,I)-(EPS(J,1)/2.+EPS(J,2)/2.)*(ANU1+ANU2)*E
104   IF(I.NE.1)  GO TO 103
      SIG(K1,J)=SIGMA(K1,I)
103   CONTINUE
      IF (NSTR.EQ.1) GO TO 905
      PRINT 707,J,(( SIGMA(K1,I),K1=1,3),I=2,NSTR)
707   FORMAT(I5,6X,12E10.3)
905   IF(ICR(J).EQ.0)  GO TO 906
      ICR(J)=ICR(J)+1
      GO TO   101
906   PP1=(SIG(1,J)+SIG(2,J))/2.
      PP2=(SIG(1,J)-SIG(2,J))/2.
      PP3=SQRT(PP2*PP2+SIG(3,J)*SIG(3,J))
      SIGP1=PP1+PP3
      SIGP2=PP1-PP3
      THETA=(ATAN2(SIG(3,J),PP2))*90./PI
      IF(SIGP1-SIGCR)  15,16,16
16    ICR(J)=1
      KCR=KCR+1
15    PRINT 18,J,ICR(J),(SIG(I,J),I=1,3),SIGP1,SIGP2,THETA
18    FORMAT(2I5,2X,3E13.4,2X,2E13.4,F10.4/)
101   CONTINUE
      DO 201 I=1,NT1
      J=1
211   NC=0
      IJ=I+(J-1)*NT1
      IF (ICR(IJ).NE.1) GO TO 212
      IF(ICR(IJ-NT1).GT.1)  GO TO 219
215   IN=IJ+NT1
      IF(IN.GT.KT) GO TO 204
      IF(ICR(IN).NE.1) GO TO 204
      NC=NC+1
      IJ=IN
      GO TO 215
204   IF(NC.EQ.0) GO TO 216
      NC1=NC
      IF(ICR(IN).LE.1)  GO TO 231
      ICR(IJ)=0
      IJ=IJ-NT1
      NC1=NC-1
231   IF(NC.EQ.1)  GO TO 217
      PMAX=(SIG(1,IJ)+SIG(2,IJ))/2.+SQRT ((SIG(1,IJ)-SIG(2,IJ))*(SIG(1,
```

```
     1IJ)-SIG(2,IJ)) /4.+SIG(3,IJ)*SIG(3,IJ))
      IJC=IJ
      ICR(IJ)=0
      DO 210 NN=1,NC1
      IJ=IJ-NT1
      ICR(IJ)=0
      PRS =(SIG(1,IJ)+SIG(2,IJ))/2.+SQRT ((SIG(1,IJ)-SIG(2,IJ))*(SIG(1,
     1IJ)-SIG(2,IJ)) /4.+SIG(3,IJ)*SIG(3,IJ))
      IF(PMAX.GT.PRS) GO TO 210
      PMAX=PRS
      IJC=IJ
  210 CONTINUE
      KCR=KCR-NC
      ICR(IJC)=1
      GO TO 218
  216 IF(ICR(IN).LE.1)  GO TO 217
      ICR(IJ)=0
      KCR=KCR-1
  217 KCR=KCR-NC
  218 J=J+1+NC
      GO TO 212
  219 ICR(IJ)=0
      KCR=KCR-1
  212 J=J+1
      IF(J.LT.MT1) GO TO 211
  201 CONTINUE
      NCRT=NCRT+KCR
      PRINT 239
  239 FORMAT(≠ ELEMENTS CRACKED THIS ROUND,  TOTAL CRACKED≠)
      PRINT19,KCR,NCRT
  19  FORMAT(I14,I25)
      IF (NSELT.EQ.0) GO TO 13
      PRINT 603
  603 FORMAT(1H1)
      PRINT 601
  601 FORMAT (≠  STEEL ELEMENT≠,≠        STRESS≠)
      LST2=2*LFSN-1
      DO 600 I=1,NSELT
      LST1=LST2
      LST2=LST1+2*NT
      SIGST(I)=(ELD(LST2)-ELD(LST1))*ES/DX
      PRINT 602,I,SIGST(I)
  602 FORMAT (I15,F13.4)
  600 CONTINUE
  13  IF(KCR.NE. 0) GO TO 22
  4   CONTINUE
      PRINT 777
  777 FORMAT(≠     END OF PROBLEM≠)
      NPRLM=NPRLM-1
      IF(NPRLM.NE.0)  GO TO 1000
      STOP
      END
$ENTRY

DATA DECK

$STØP
```

OTHER PUBLICATIONS IN RELATED FIELDS BY THE ENGINEERING EXPERIMENT STATION

Bulletin 497. *Investigation of Prestressed Reinforced Concrete for Highway Bridges, Part V: Analysis and Control of Anchorage-Zone Cracking in Prestressed Concrete*, W. A. Welsh, Jr. and M. A. Sozen. 1968. $3.00.

Bulletin 498. *Prediction of Creep in Sturctural Concrete*, E. M. Wallo and C. E. Kesler. 1968. $3.00

Bulletin 499. *Fatigue of Concrete*, J. P. Lloyd, J. L. Lott, and C. E. Kesler. 1968. $2.00.

These publications are available from:

Engineering Publications Office
112 Engineering Hall
University of Illinois
Urbana, Illinois 61801

PUBLICATIONS OF THE COLLEGE OF ENGINEERING

Bulletins from the University of Illinois College of Engineering are detailed reports of research results, seminar proceedings, and literature searches. They are carefully reviewed before publication by authorities in the field to which the material pertains, and they are distributed to major engineering libraries throughout the world. They are available at a charge approximately equal to the cost of production.

The annual *Summary of Engineering Research* is available in the fall of each year. It contains a short report on every research project conducted in the College during the past fiscal year, including the names of the researchers and the publications that have resulted from their work.

Engineering Outlook, the College's monthly newsletter, contains short articles about current happenings, new research results, recent technical publications, and educational practices in the College of Engineering. Free subscriptions are available upon request.

The Seminar and Discussion Calendar, which is published and distributed weekly, lists current meetings, lectures, and other events on the engineering campus that are open to the public. Free subscriptions are available upon request.

Requests for a catalog of available technical bulletins or for any of the above publications should be addressed to the Engineering Publications Office, College of Engineering, University of Illinois, Urbana, Illinois 61801.